Nitric Oxide Regulates the *Ralstonia solanacearum* Type 3 Secretion System

Connor G. Hendrich[1], Alicia N. Truchon[1], Beth L. Dalsing[1,2], and Caitilyn Allen[1*]

[1] Department of Plant Pathology, University of Wisconsin – Madison, Madison, Wisconsin, USA

[2] Present address: Syngenta, Durham, NC

[*] Corresponding author: Caitilyn Allen, E-mail: callen@wisc.edu

Keywords: *Ralstonia solanacearum*, Type III Secretion, nitric oxide, bacterial wilt, vascular wilt, tomato

Funding: National Sciences Foundation grant IOS 1258082.

23 **Abstract**

24

25 *Ralstonia solancearum* causes bacterial wilt disease on diverse plant hosts. *R.*
26 *solanacearum* cells enter a host from soil or infested water through the roots, then
27 multiply and spread in the water-transporting xylem vessels. Despite the low nutrient
28 content of xylem sap, *R. solanacearum* grows very well inside the host, using
29 denitrification to respire in this hypoxic environment. *R. solanacearum* growth *in planta*
30 also depends on the successful deployment of protein effectors into host cells via a
31 Type III Secretion System (T3SS). The T3SS is absolutely required for *R. solanacearum*
32 virulence, but it is metabolically costly and can trigger host defenses. Thus, the
33 pathogen's success depends on optimized regulation of the T3SS. We found that a
34 byproduct of denitrification, the toxic free-radical nitric oxide (NO), positively regulates
35 the *R. solanacearum* T3SS both *in vitro* and *in planta*. Using chemical treatments and
36 *R. solanacearum* mutants with altered NO levels, we show that the expression of a key
37 T3SS regulator is induced by NO in culture. Analyzing the transcriptome of *R.*
38 *solanacearum* responding to varying levels of NO both in culture and *in planta* revealed
39 that the T3SS and effectors were broadly upregulated with increasing levels of NO. This
40 regulation was specific to the T3SS and was not shared by other stressors. Our results
41 suggest that *R. solanacearum* experiences an NO-rich environment in the plant host
42 and may use this NO as a signal to activate T3SS during infection.

43

Keywords: *Ralstonia solanacearum*, Type III Secretion, nitric oxide, bacterial wilt, vascular wilt, tomato

Introduction

Ralstonia solancearum (*Rs*) is a Gram-negative soil-borne betaproteobacterium that causes bacterial wilt disease on a wide range of plant hosts, including important crops like tomato, potato, and banana (Elphinstone 2005). The bacteria survive in and are spread through infected soil and water, infecting host roots through wounds and natural openings (Vasse et al. 1994). Once inside, *R. solanacearum* cells move to the xylem, where they can grow and spread throughout the plant. Although this bacterium is slow growing and sensitive to stress when grown *in vitro*, in plant xylem vessels *R. solanacearum* is a formidable force. *R. solanacearum* quickly grows to high cell densities in xylem even though this habitat is low in oxygen and nutrients, and accessible to host defenses (Genin and Denny 2012). As it grows, *R. solanacearum* produces an arsenal of virulence factors, including highly mucoid extracellular polymeric substances (EPS), a consortium of cell wall degrading enzymes, and dozens of protein effectors that are injected into host cells via the Type III Secretion System (T3SS) (Genin and Denny 2012). Water transport in infected plants is eventually blocked by a combination of host-produced gels and tyloses, degradation of vessel walls, EPS, and the sheer mass of bacterial cells. Without sufficient water, plants wilt and die while *R. solanacearum* cells escape back into the soil, where they can find another host (Swanson et al. 2007).

65 The lethality of bacterial wilt disease combined with its wide host range and a
66 lack of effective treatments make *R. solanacearum* an important agricultural problem
67 around the world (Yuliar et al. 2015; Elphinstone 2005). Successful disease
68 management depends on understanding *R. solanacearum* biology, but the pathogen
69 behaves very differently in culture than it does in its natural environment (Jacobs et al.
70 2012). In particular, the T3SS, which is absolutely essential for virulence and subject to
71 a complex regulatory cascade, is affected by the plant environment in ways that remain
72 poorly understood (Poueymiro and Genin 2009). The PhcA quorum sensing system
73 upregulates T3 secretion in culture, but not *in planta* (Génin et al. 2005; Jacobs et al.
74 2012; Monteiro et al. 2012a; Khokhani et al. 2017). An unidentified 'diffusible factor'
75 increases T3SS expression *in planta* via the HrpG global regulator (Genin and Denny
76 2012).

77 We have discovered that the diffusible free radical nitric oxide (NO) plays a role
78 in *R. solanacearum* life inside plants. Xylem sap is rich in nitrate, which *R.*
79 *solanacearum* uses as an alternate electron acceptor to respire in the hypoxic xylem
80 environment (Dalsing et al. 2015). The *R. solanacearum* strain GMI1000 reduces nitrate
81 completely to dinitrogen gas by means of denitrifying respiration. The genes required for
82 this process are highly expressed during infection (Jacobs et al. 2012; Khokhani et al.
83 2017). However, denitrifying respiration produces NO as an intermediate. In large
84 quantities, NO is toxic and strongly inhibits *R. solanacearum* growth. The pathogen
85 manages this threat by detoxifying NO with the nitric oxide reductase NorB and the
86 flavohemoglobin HmpX, which are both highly expressed *in planta* and required for full

87 virulence (Dalsing et al. 2015; Jacobs et al. 2012). Plants use NO extensively for both
88 signaling and defense, and can produce NO through multiple different pathways
89 (Scheler et al. 2013; Delledonne et al. 1998; Simontacchi et al. 2015; Wilson et al. 2008;
90 Leitner et al. 2009). Thus, *R. solanacearum* likely encounters NO during plant
91 pathogenesis.

92 In this study, we identify a link between NO and regulation of the *R.*
93 *solanacearum* T3SS. We first show that T3SS gene expression increases when *R.*
94 *solanacearum* is actively denitrifying. We then show that this effect depends specifically
95 on the presence of NO. Based on these results, we conducted a transcriptomics
96 experiment to determine the effects of NO on *R. solanacearum* gene expression in
97 culture and *in planta* and show that levels of many transcripts, including 107 T3SS-
98 related genes, are altered by changes in NO levels.

99

100 **Results**

101 **Nitric oxide changes expression of the *R. solanacearum* T3SS**

102 Regulation of the T3SS in *R. solanacearum* is multi-layered and incompletely
103 understood (Fig 1.A). Because *R. solanacearum* actively denitrifies *in planta*, we
104 wondered if this pathway or its products affect T3SS expression during plant infection
105 (Dalsing et al. 2015; Jacobs et al. 2012). To test this hypothesis, we used an *R.*
106 *solanacearum* reporter strain carrying a fusion of the *lux* operon to the promoter of *hrpB*,
107 which encodes a key T3SS regulator (Genin and Denny 2012). Transcription of *hrpB*
108 increased >3-fold when the bacterium was denitrifying in culture (Fig. 1B).

109 An intermediate product of denitrification is the highly reactive free radical NO.
110 Because NO is a common signaling molecule in eukaryotes, we decided to determine if
111 it was responsible for *hrpB* activation observed during denitrification. To block the
112 effects of NO, we used the NO-scavenging chemical cPTIO (Pfeiffer et al. 1997). While
113 cPTIO is commonly used to both detect and deplete NO from solutions, it can also be
114 reduced or inactivated by factors other than NO (D'Alessandro et al. 2013). To mitigate
115 cPTIO effects unrelated to NO, we tested its ability to affect *hrpB* expression in two
116 conditions. First, we incubated *R. solanacearum* in denitrification-promoting conditions
117 with and without cPTIO. We measured *hrpB* expression in RNA extracted from these
118 cultures at 16 hpi, near the peak of *hrpB::lux* expression. In these conditions, NO
119 scavenging by cPTIO slightly but significantly reduced *hrpB* expression (Fig. 1C). We
120 then tested the effect of a host on the interaction between *hrpB* expression and NO. We
121 incubated a cell suspension of R. solanacearum *hrpB::lux* with tomato seedlings for 24
122 hours with or without cPTIO. As expected, the presence of a host plant activated *hrpB*
123 gene expression. However, adding cPTIO to the mixture completely reversed this effect
124 (Fig. 1D). Together, these results indicated that the denitrifying respiration-dependent
125 increase in *hrpB* expression observed in culture is specifically triggered by NO. Further,
126 this result suggests that NO could be the unknown soluble signal that increases *hrp*
127 regulon expression *in planta*.

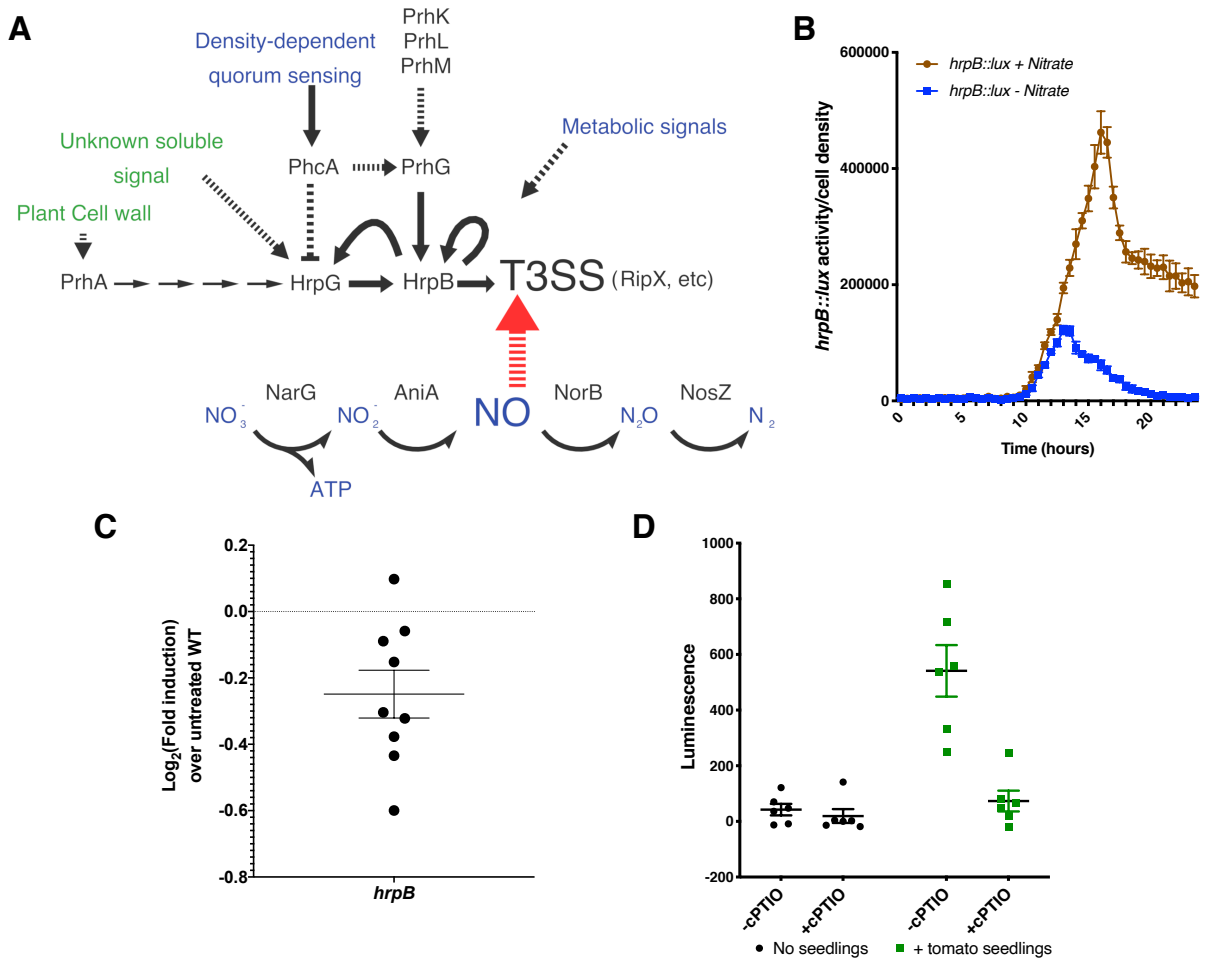

Fig. 1. Nitric oxide affects expression of the *R. solanacearum* T3SS. **A,** Summary of known T3SS regulation in *R. solanacearum* strain GMI1000. Arrows indicate positive regulation, barred lines indicate repression, dashed lines indicate an unknown or uncharacterized mechanism, green text indicates plant-derived signals, and blue text indicates metabolites. T3SS genes, such as the T3 effector *ripX*, are controlled by the transcriptional regulator HrpB. HrpB is transcriptionally activated by HrpG and PrhG, which are themselves controlled by the quorum-sensing regulator PhcA, but only *in vitro*. PrhG activity also depends on three uncharacterized proteins, PrhK, PrhL, and PrhM, through an unknown mechanism. HrpG is activated by the contact-dependent

138 plant cell wall sensor PrhA as well as by an unknown soluble signal present during plant
139 infection. **B,** Expression of a bacterial luciferase transcriptional reporter of HrpB. *R.*
140 *solanacearum* strain GMI1000 *hrpB::lux* was grown in denitrification-inducing conditions
141 with or without 30 mM nitrate. Both culture density (OD_{600}) and luminescence were
142 measured every 30 min, and luminescence was normalized to culture density. Error
143 bars represent standard error of the mean. Cultures grown with nitrate had significantly
144 increased *hrpB* expression (2-way ANOVA, P=0.0003). **C,** The NO scavenger cPTIO
145 reduces *hrpB* expression in *R. solanacearum* cells grown in denitrifying conditions.
146 Cultures were grown as in B with and without 1 mM cPTIO and harvested at 16 hpi.
147 *hrpB* expression was measured using qRT-PCR. Expression of *hrpB* was reduced in
148 cPTIO-treated cultures (P<0.0001, students T test) Error bars represent standard error
149 of the mean. **D,** The NO scavenger cPTIO decreased T3SS activity in the presence of a
150 host. Luminescence of *R. solanacearum hrpB::lux* was measured after 24 h incubation
151 in water with or without five day-old tomato seedlings, and with or without 1 mM cPTIO,
152 an NO-scavenger. Exposure to tomato seedlings induced *hrpB::lux* expression
153 (P=0.004, students T test). *R. solanacearum* cells exposed to both tomato seedlings
154 and cPTIO had luminescence indistinguishable from that of cells without tomato
155 seedlings. Error bars represent standard error of the mean.
156
157 **Denitrifying metabolism causes broad changes in *R. solanacearum* gene**
158 **expression.**

159 While the above results showed that NO can affect *hrpB* expression, many other
160 genes are involved in regulation, biosynthesis, and function of the *R. solanacearum*
161 T3SS. To better understand the broader effects of NO on pathogen biology and T3SS
162 gene expression, we sequenced the transcriptomes of *R. solanacearum* cells grown
163 with varying levels of NO both in culture and in infected tomato plants (Fig. 2A). In
164 culture, we grew the cells in 0.1% O_2 in a modified Van den Mooter medium (VDM),
165 which promotes denitrifying respiration (Dalsing et al. 2015). We manipulated
166 intracellular *R. solanacearum* NO levels genetically by using mutants lacking either the
167 NarG nitrate reductase (the *ΔnarG* mutant cannot denitrify and does not produce NO),
168 or the NorB nitric oxide reductase (the *ΔnorB* mutant accumulates NO, see
169 Supplementary Fig. 1). Exogenous NO levels were manipulated by treating cells with
170 CysNO, a nitrosothiol NO donor. Because high NO levels are toxic to *R. solanacearum*,
171 we controlled for general stress responses by also profiling transcriptomes of cultures
172 treated with H_2O_2, a non-NO source of stress. After about 18 h, growth of the *ΔnorB*
173 mutant was inhibited by accumulating NO, so we sampled cultures 16 hpi, when *ΔnarG*,
174 *ΔnorB*, and the wild-type strain were at similar densities (Supplementary Fig. 1). CysNO
175 or H_2O_2 treatments were added 4 h before sampling, at the highest concentrations that
176 did not significantly alter culture growth (Supplementary Fig 2A). Total RNA was
177 extracted from bacteria *in planta* 3 days after tomato plants were inoculated with ~2000
178 CFU of *R. solanacearum* through a cut petiole (Khokhani et al. 2017). This method
179 synchronized the infection process better than root inoculation. Bacterial colonization in
180 sampled tissue was standardized by extracting RNA only from stems containing

181 between 5x10^7 and 10^9 CFU/g stem, as determined by dilution plating a ground stem

182 section (Supplementary Fig. 2B). Each of the three biological replicates contained

183 pooled RNA from 4 or 5 plants.

184

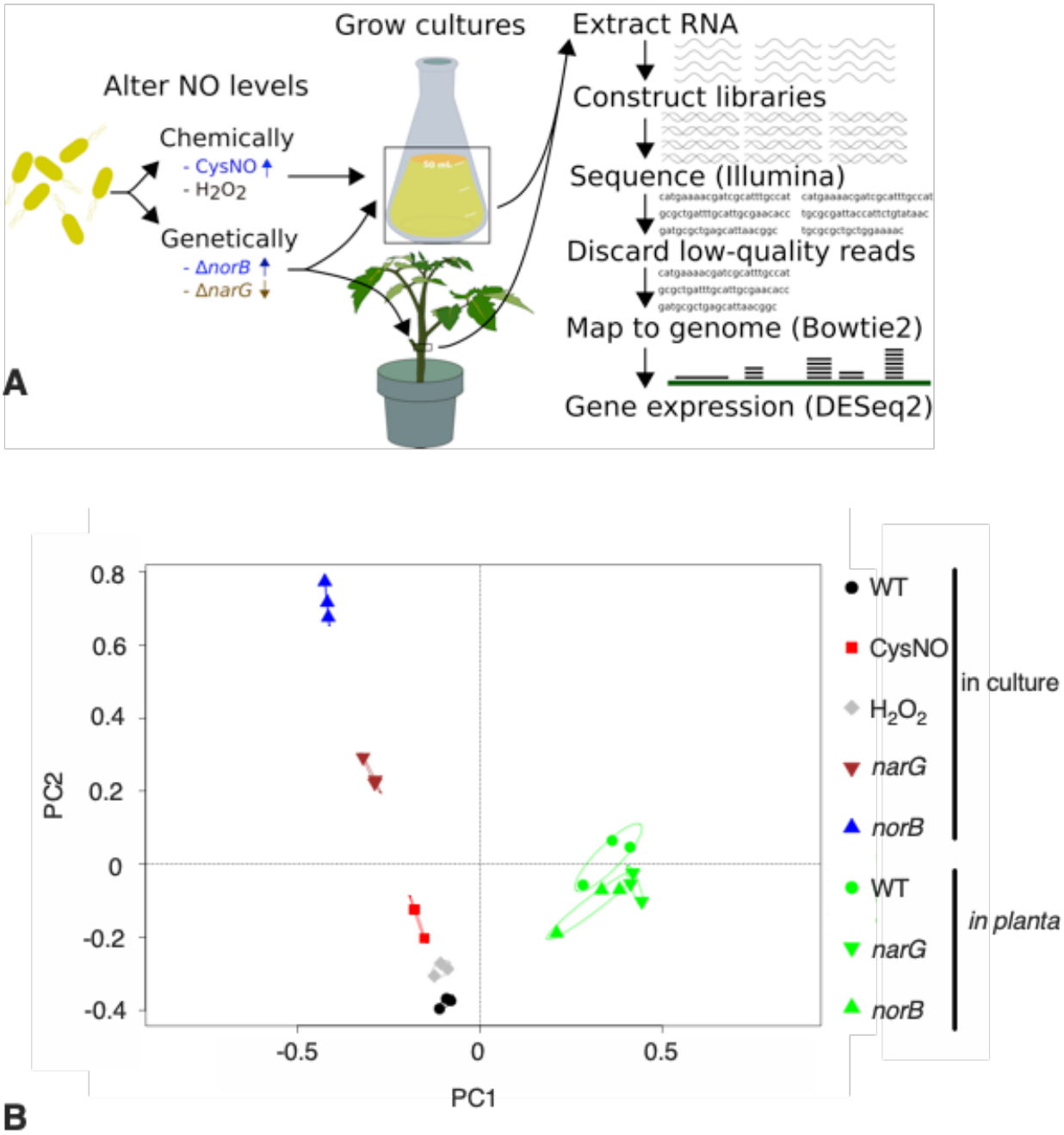

185

186 **Fig. 2.** Nitric oxide causes broad changes in *R. solanacearum* gene expression. **A,**
187 Design of RNA-seq experiment. We extracted RNA from *R. solanacearum* grown with
188 altered NO levels from stems of infected tomato plants (*in planta)* and from denitrifying
189 VDM medium (in culture) and NO levels were increased chemically by adding the NO
190 donor CysNO to wild type (WT) and increased genetically by using a NO-accumulating
191 *Δ*norB mutant. The *ΔnarG* mutant has reduced levels of NO. H_2O_2 -treated WT was
192 included as a control for non-nitrosative general stress responses. **B,** Whole-
193 transcriptome datasets were used for principal component analysis; plot created in R
194 with the package Vegan (Oksanen et al. 2019). Each data point represents one
195 biological replicate, with three replicates per condition. Ellipses represent a 95%
196 confidence interval for each condition (some ellipses are so small that they appear as
197 lines).
198
199 Around 97% of RNA-seq reads from *in vitro* samples mapped to the *R.*
200 *solanacearum* genome (Supplementary Fig. 3A). Because tomato stem slices also
201 included host RNA, only 9.2% of the *in planta* RNA reads mapped to the *R.*
202 *solanacearum* genome. However, the absolute number of bacterial transcripts from the
203 *in planta* samples still exceeded 10^6 reads per replicate. Principal component analysis
204 clustered the *in vitro* samples together based on treatment, and the *in planta* samples
205 were even more tightly clustered, reflecting less variation in gene expression than the
206 culture samples (Fig. 2B). Genes were considered differentially expressed if they had

207 an adjusted P-value <0.05. A full list of gene expression values can be found in the
208 supplementary materials.

209 We validated our transcriptomic results by using qRT-PCR to measure the
210 expression of two regulators of T3SS, *hrpB* and *hrpG*, and one well-expressed T3E,
211 *ripX*. Expression levels of each of these genes in the *ΔnarG* and *ΔnorB* mutants
212 generally matched those obtained from RNA-seq analysis (Fig. 3). As with *hrpB*
213 expression, *hrpG* and *ripX* were both activated by NO, whether it was produced
214 endogenously or exogenously.

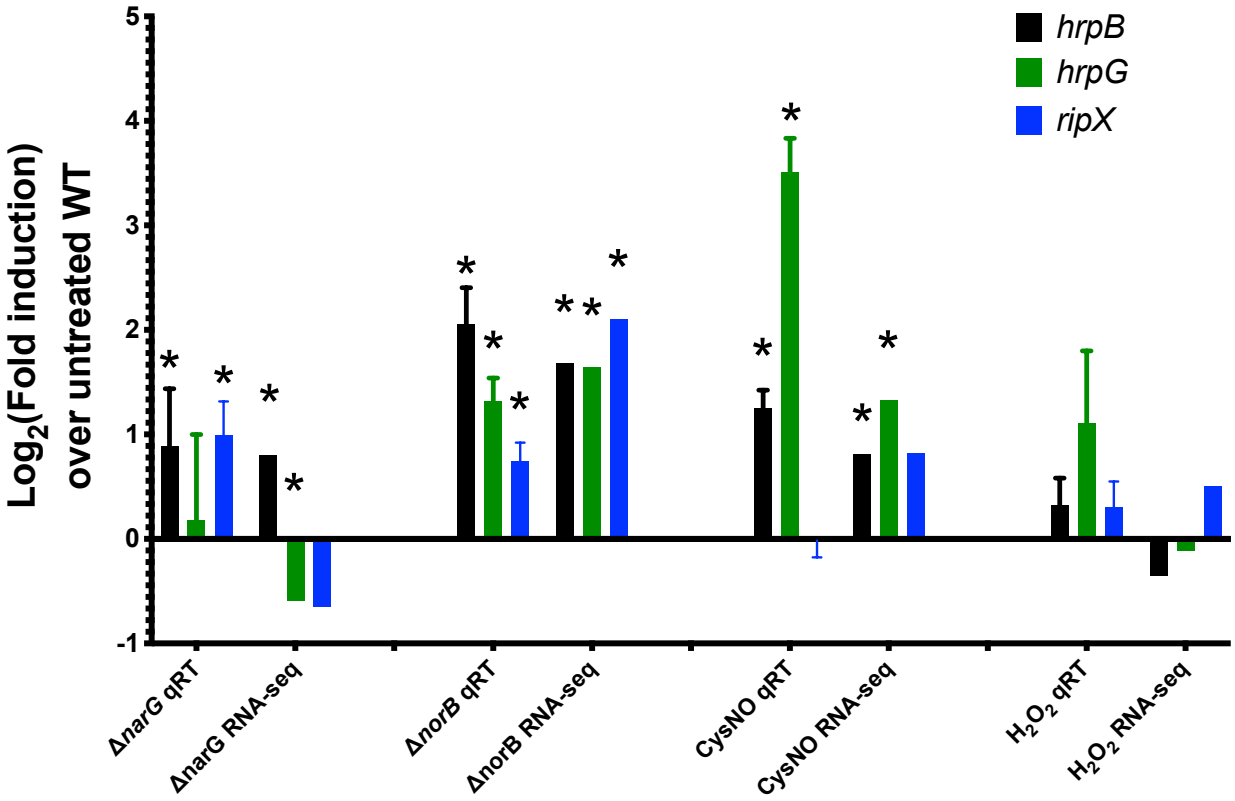

215

216 **Fig. 3.** Expression analysis of selected T3SS-related genes by qRT-PCR validated
217 RNA-seq results. RNA was extracted from *R. solanacearum* cultured in VDM media at
218 0.1% oxygen for 16 hours for both qRT-PCR and RNA-seq analysis. *R. solanacearum*

219 samples were: wild type strain GMI1000 (WT, untreated control reference), non-
220 denitrifying low-NO mutant *(ΔnarG*) and NO-accumulating mutant (*ΔnorB*), and WT
221 treated for 4h with exogenous NO (CysNO). Gene expression levels in all samples were
222 normalized using *serC* (Jacobs et al. 2012). Error bars indicate standard error of the
223 mean. Black bars, log_2fold-change expression of T3SS regulatory gene *hrpB;* green
224 bars*,* log_2 fold-change expression of T3SS regulatory gene *hrpG;* blue bars*,* log_2 fold-
225 change expression of Type 3-secreted effector gene *ripX.* * $P<0.05$, for qRT, student's
226 t-test compared to gene expression level in untreated WT bacteria; for RNA-seq, FDR
227 using Benjamini-Hochberg.
228

229 **Denitrifying conditions in culture do not replicate *in planta* conditions**

230 Because xylem fluid contains relatively small amounts of nutrients, minimal
231 media has often been considered to mimic the xylem environment (Arlat et al. 1992;
232 Lowe-Power et al. 2018a). Because VDM is a minimal medium and *R. solanacearum*
233 experiences low-oxygen conditions and uses denitrifying respiration during tomato
234 infection, we asked if anaerobic growth in VDM would better mimic the tomato xylem
235 environment than rich media (Dalsing et al. 2015). However, when we examined
236 expression of *R. solanacearum* genes in tomato stems compared to in VDM, we found a
237 total of 1038 genes were differentially regulated in these conditions (Supplementary
238 Table 2). Most genes involved in denitrification were expressed at a higher level in VDM
239 than *in planta*. Other broad categories that were altered include sugar metabolism,
240 flagellar motility, amino acid transporters, iron uptake genes, and ribosomal proteins. In

241 line with previous results, T3SS-related genes were among the most highly upregulated
242 genes *in planta* (Jacobs et al. 2012). Overall, growth in VDM did not closely replicate
243 the *in planta* environment and the bacterium seemed more reliant on denitrifying
244 metabolism in VDM.
245

246 **Altering denitrification and NO levels changes expression of denitrification and**
247 **virulence-related genes *in planta***

248 To determine if the effects of NO on the T3SS were specific or a part of a non-
249 specific general response, we examined genes differentially regulated the non-
250 denitrifying *ΔnarG* and NO-accumulating *ΔnorB in planta*. In the stem, 187 genes were
251 significantly altered by mutating *narG* and thus blocking denitrification and NO
252 production, while only 49 genes were altered in the NO accumulating *ΔnorB* mutant. In
253 *ΔnarG*, nine of the most significantly upregulated genes were directly involved in nitrate
254 sensing and uptake or were components of the nitrate reductase protein. In both *ΔnarG*
255 and *ΔnorB*, genes involved in motility and sulfur metabolism were decreased compared
256 to WT (Supplementary Table 2). Overall, this muted response highlights the robust
257 regulatory state of *R. solanacearum* cells growing *in planta* and shows that they can
258 tolerate even changes in fundamental aspects of its biology (Peyraud et al. 2018).

259 Consistent with the observation that the entire transcriptome of WT *R.*
260 *solanacearum* was very different *in planta* than in culture (Fig. 2aA) the transcriptomic
261 profiles of the denitrification mutants grown in culture were much more divergent from
262 that of WT, with 3,145 significantly altered genes in *ΔnarG* and 3,976 altered in *ΔnorB*.

263 In the non-denitrifying *ΔnarG*, the bacterium showed decreased expression in many
264 KEGG pathways involved in growth and metabolic activity such as purine and
265 pyrimidine metabolism, oxidative phosphorylation, and tRNA synthetases
266 (Supplementary Table 3).

267 In culture, genes up-regulated in the NO-accumulating *ΔnorB* mutant were
268 enriched in the KEGG pathways of flagellar assembly, sulfur relay system and fatty acid
269 degradation (Supplementary Table 3). Downregulated genes were enriched in central
270 metabolic KEGG pathways like oxidative phosphorylation, pyrimidine metabolism,
271 biosynthesis of amino acids, and fatty acid biosynthesis. In contrast to the activation of
272 the T3SS, CysNO-treated *R. solanacearum* cells and *ΔnorB* saw reduction in
273 expression of Types I, II, and VI secretion systems. Overall, the transcriptomic
274 responses of *Rs* cells to either increased or decreased NO did not align well with their
275 responses *in planta*. This is consistent with previous studies showing that cultured *Rs*
276 cells do not reflect biology of the pathogen in its natural habitat (Jacobs et al. 2012;
277 Perrier et al. 2018).

278

279 **_R. solanacearum_ encounters more nitrosative stress in VDM than _in planta_**

280 To estimate the degree of nitrosative stress induced by our treatments, we
281 looked at the expression of *norB* and *hmpX*, which directly detoxify NO in *R.*
282 *solanacearum* (Farr and Kogoma 1991; Dalsing et al. 2015). Compared with *R.*
283 *solanacearum* growing in denitrifying culture conditions, *norB* and *hmpX* expression
284 decreased 5-fold and 20-fold *in planta*, suggesting that in this environment the

285 bacterium experiences lower nitrosative stress levels (Supplementary Table 2). In
286 striking contrast, expression of the oxidative stress-response catalase gene *katE* was
287 increased 35-fold *in planta*. *In planta*, neither the non-denitrifying *ΔnarG* strain nor the
288 NO overproducing *ΔnorB* strain showed significant changes *norB* or *hmpX* expression.
289 Conversely, the *ΔnorB* mutant grown in culture had an 11-fold up-regulation of the NO-
290 detoxifying *hmpX*. In culture, our oxidative stress control treatment with H_2O_2 increased
291 expression of *katE*, as expected, but also had increased expression of NO detoxifying
292 genes *hmpX* and *norB*. Overall, these results showed some overlap in the response to
293 ROS and RNS stress in culture but suggested that *R. solanacearum* cells experienced
294 less nitrosative stress in tomato xylem than when denitrifying in VDM culture.
295

296 **Nitric oxide induced expression of T3SS-related genes both *in vitro* and *in planta*.**

297 To determine if in addition to *hrpB*, other T3SS-associated genes are induced by
298 NO in culture, we measured relative expression of all 107 known *R. solanacearum*
299 T3SS genes under each tested condition. These genes encode T3SS structural
300 elements, regulators, secreted effectors, and chaperones (Fig. 4) (Cunnac et al. 2004;
301 Peeters et al. 2013; Van Gijsegem et al. 1995; Plener et al. 2010; Lonjon et al. 2017;
302 Zhang et al. 2015b, 2018, 2011; Brito et al. 1999; Marc Marenda et al. 1998; Lonjon et
303 al. 2015; Génin et al. 2005). Cells of the NO-accumulating *ΔnorB* mutant grown in
304 culture had broadly increased T3SS gene expression relative to wild type, with nine of
305 sixteen structural elements significantly increased. Only one structural element, *hrpF*,
306 trended non-significantly towards reduced expression (Fig. 4A). Five out of thirteen

307 known regulators of T3SS were significantly upregulated in *ΔnorB*, although expression
308 of the *prhA*, *prhG*, *prhO*, and the *prhKLM* operon were all reduced. Two out of the four
309 T3E chaperones had significantly elevated expression in *ΔnorB*, as did most T3Es. The
310 differential expression of effectors did not seem to correlate with their known
311 interactions with chaperones (Supplementary Table 4). The expression of T3SS genes
312 in CysNO-treated cells largely mirrored that of *norB*, with 80% of tested genes having a
313 similar trend. However, the magnitude of the effect was lower. T3SS gene expression in
314 *ΔnarG* was more varied, with fewer significantly differentially regulated genes than
315 *ΔnorB*. In contrast to *ΔnorB*, *ΔnarG*, and CysNO-treated cultures, H_2O_2-treated cultures
316 had only eight significantly changed T3SS genes (Fig. 4A). Overall, we saw a greater
317 induction of T3SS genes in culture by our high-NO conditions than low-NO conditions.

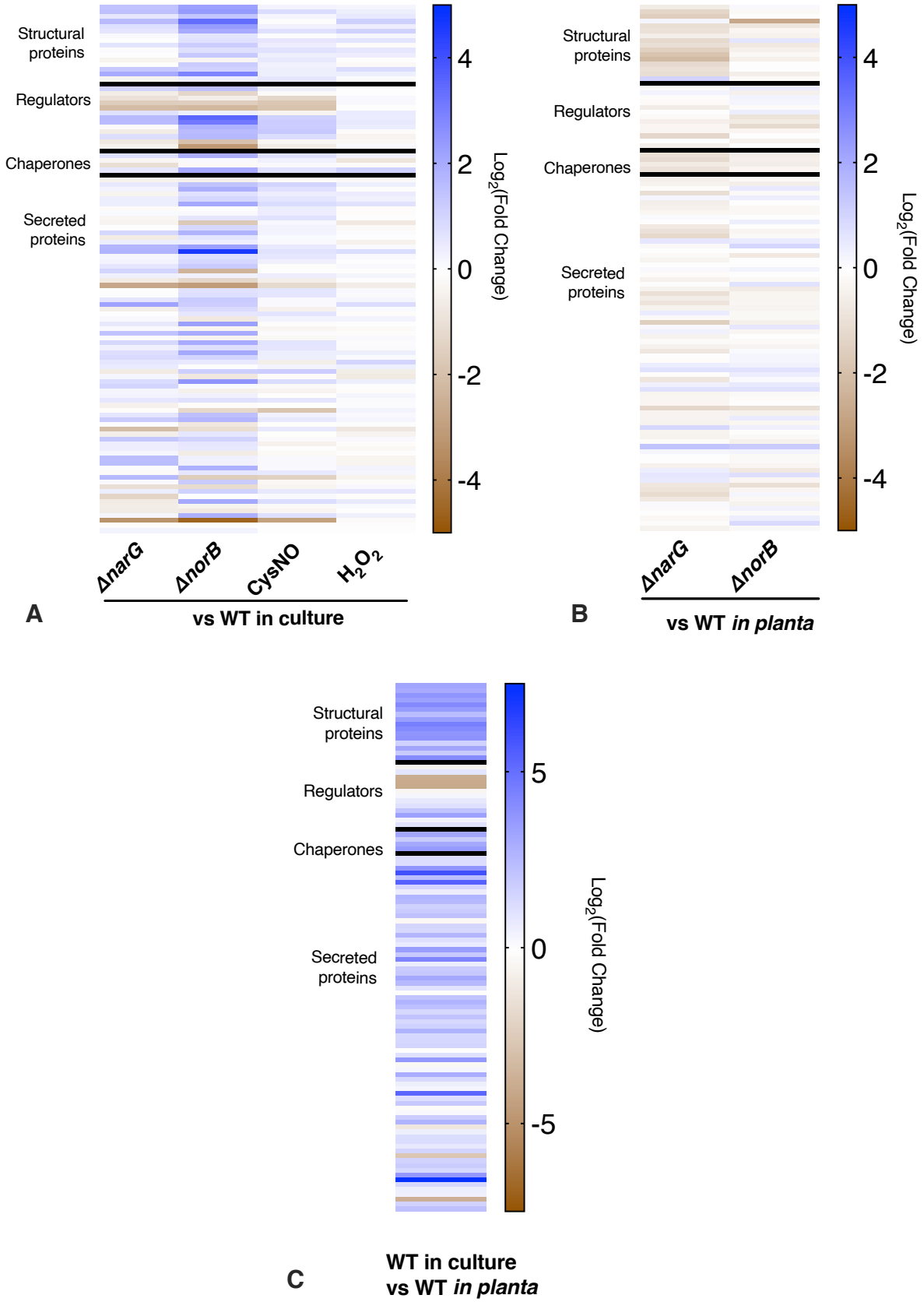
Structural proteins
Regulators
Chaperones
Secreted proteins
ΔnarG
ΔnorB
CysNO
H2O2
A
vs WT in culture
4
2
0
-2
-4
Log2(Fold Change)
B
vs WT in planta
C
WT in culture
vs WT in planta
5
-5

319 **Fig. 4.** Nitric oxide alters expression of T3SS-related genes both *in vitro* and *in planta*.
320 **A,** Heatmap showing relative expression levels of 107 T3SS-associated genes in *R.*
321 *solanacearum* cells growing in rich medium with varying NO levels. All fold-change
322 numbers are compared to levels in untreated wild-type (WT) cells. Gene annotations,
323 fold change, and significance levels can be found in the supplementary materials. NO
324 levels were modified genetically using mutants lacking *narG* (deleting this nitrate
325 reductase reduces endogenous NO) and *norB* (deleting this nitric oxide reductase
326 increases endogenous NO). NO levels were increased chemically by adding 1 mM
327 CysNO. Cells treated with 100 μM hydrogen peroxide (H_2O_2) were a non-NO control to
328 show general stress responses. **B,** Relative expression levels of 107 T3SS-associated
329 genes in *R. solanacearum* cells growing *in planta*. About 2000 CFU of WT *R.*
330 *solanacearum, ΔnarG*, or *ΔnorB* were introduced into 17-day old Bonny Best tomato
331 plants through a cut petiole and RNA was harvested from a stem slice 3 days after
332 inoculation. **C,** Expression of most T3SS-associated genes in *R. solanacearum* strain
333 GMI1000 was enhanced when the bacterium grew in tomato plants relative to when *R.*
334 *solanacearum* cells multiplied *in vitro* under denitrifying conditions (VDM medium, 0.1%
335 O_2).
336
337 To determine if altering NO levels affects *R. solanacearum* T3SS gene
338 expression in a biologically relevant environment with all natural T3SS regulating inputs,
339 we examined changes in T3SS gene expression in *ΔnarG* and *ΔnorB in planta*.
340 Compared to *R. solanacearum* grown in culture, wild type *R. solanacearum in planta*

341 had much higher expression of almost every T3SS-associated gene (Fig. 3C). When
342 growing in tomato stems, *ΔnorB* grown *in planta* had no significantly differentially
343 regulated T3SS genes, possibly because relatively high levels of NO are already
344 present in the plant environment (Fig. 3B). In contrast, the non-denitrifying *ΔnarG*
345 mutant showed an overall trend of lower T3SS gene expression, with expression of nine
346 genes significantly reduced (Fig. 3B). These included two components of the T3SS
347 structure, *hrpF* and *hrcN*, the regulators *hrpB* and *prhG*, the effector chaperone *hpaG*,
348 and four T3SS effectors. Even in the highly T3SS-inducing *in planta* environment,
349 reducing *R. solanacearum*-produced NO was sufficient to reduce T3SS gene
350 expression in tomato xylem.
351

352 **Discussion**

353 The T3SS is essential for *R. solanacearum* virulence, as it is for many Gram-
354 negative pathogenic bacteria. Involving at least 16 structural proteins, this secretion
355 system is metabolically expensive to synthesize and operate, so the bacterium is under
356 strong selection pressure to express it only when it increases fitness (Genin et al. 1992;
357 Boucher et al. 1985). Many factors contribute to the regulation of T3SS in *R.*
358 *solanacearum*, including the presence of undefined host cell wall materials, unknown
359 soluble factors, unknown metabolic cues, and (in culture) quorum sensing (Zuluaga et
360 al. 2013; Brito et al. 1999; Aldon et al. 2000; Genin and Denny 2012; Zhang et al. 2018,
361 2011; Senuma et al. 2020). While many T3SS regulators have been described, open
362 questions remain, such as why T3SS is repressed in rich media and whether specific

363 host cell wall components activate PrhA. In addition, many genes that affect T3SS gene
364 expression do so via unknown mechanisms (Zhang et al. 2011, 2015b, 2018). The
365 results presented here suggest that NO participates in this complex regulatory network.
366 Despite its toxicity at high concentrations, NO is widely used as a signaling
367 molecule in all domains of life (Asgher et al. 2017; Astuti et al. 2018; Simmonds et al.
368 2014). Many effects of NO are mediated by NO-dependent protein post-translational
369 modifications, including binding transition metals, S-nitrosylation of cysteine, and
370 tyrosine nitration (Simmonds et al. 2014; Cooper 1999; Leitner et al. 2009; Wünsche et
371 al. 2011; Kolbert et al. 2017; Zhang et al. 2015a; Russwurm and Koesling 2004). While
372 most well-characterized mechanisms of NO signaling have been described in
373 eukaryotes, examples of NO signaling in bacteria have also been identified. Species in
374 *Legionella*, *Shewanella*, *Vibrio*, and *Silicibacter* have been shown to use H-NOX
375 proteins to sense NO and regulate biofilm formation (Rao et al. 2015; Henares et al.
376 2012; Liu et al. 2012; Network et al. 2012; Carlson et al. 2010). NO also contributes to
377 biofilm regulation in *Pseudomonas aeruginosa* via the protein NosP (Hossain and Boon
378 2017). Both H-NOX proteins and NosP bind NO using iron centers, but no orthologues
379 of these genes are apparent in the *R. solanacearum* genome. The first example of S-
380 nitrosylation in bacteria was the oxidative stress response protein OxyR in *E. coli* (Seth
381 et al. 2012). OxyR regulates a distinct set of genes when a key cysteine is nitrosylated
382 rather than oxidized. In addition to this, nitrosative stress damage triggers S-
383 nitrosylation of the *Salmonella enterica* redox sensor SsrB and affects the S-nitroso
384 proteome of *Mycobacterium tuberculosis* (Rhee et al. 2005; Husain et al. 2010).

385 Although we show NO activates a key virulence factor in *R. solanacearum*, its specific
386 mechanism of action is not yet known. Using *in silico* predictions of NO-dependent post-
387 translational modifications, we could identify and selectively modify potentially important
388 residues in T3SS regulatory proteins to determine the mechanism of NO-dependent
389 T3SS activation (Xue et al. 2010; Liu et al. 2011).

390 We found that expression of T3SS-associated genes was enhanced by the
391 presence of a plant host and by exogenous NO released by the NO donor CysNO, and
392 the plant-mediated induction was suppressed by the NO scavenger cPTIO (Fig. 1C).
393 T3SS gene expression also increased in response to nitric oxide produced by *R.*
394 *solanacearum* itself, both at natural levels generated by denitrifying respiration and at
395 enhanced levels caused by deleting *norB*. As previously reported (Monteiro et al.
396 2012a; Jacobs et al. 2012; Khokhani et al. 2017), *R. solanacearum* cells infecting
397 tomato plants highly expressed most T3SS genes, but reducing *R. solanacearum*-
398 produced NO by preventing denitrifying respiration with a Δ*narG* mutation significantly
399 decreased expression of some T3SS-related genes *in planta*. These included genes
400 encoding structural components, HrpF and HrcN, key regulators HrpB and PrhG, the
401 chaperone HpaG, and four T3-secreted effectors (Fig. 4B). This was especially striking
402 because overall gene expression in *ΔnarG* was otherwise very similar to that of wild
403 type. These results raise the possibility that *R. solanacearum* uses the presence of NO
404 as an indirect indicator of the host xylem environment. There was no increase in T3SS
405 gene expression in the NO-overproducing *ΔnorB* mutant, which may indicate that T3SS

406 genes are already so highly expressed *in planta* that the addition of more NO does not
407 further increase this elevated level of expression.

408 Besides its effects on the T3SS, altering NO concentrations in culture elicited
409 broad changes in gene expression. We reduced NO levels using the non-denitrifying
410 mutant *ΔnarG*. However, preventing the cells from using the denitrification pathway has
411 significant effects on the biology and metabolic state of the cells, making the
412 interpretation of these results challenging. For example, the *ΔnarG* cells grown in
413 culture showed evidence of decreases in growth rate and metabolic activity, indicated
414 by decreased expression in the biosynthetic pathways of nucleotides, reduced
415 expression of the oxidative phosphorylation system, and decreased production of many
416 tRNAs. Treating the cells with NO, either with exogenously applied CysNO or with the
417 NO-overproducing *ΔnorB*, caused similar changes in many metabolic pathways in
418 culture. However, a primary force in culture was the stress caused by increased NO
419 concentrations. This manifested in decreased expression of denitrification and nitrate
420 uptake functions and an increased expression of the NO-detoxifying enzyme *hmpX*.
421 This stress was associated with decreased expression of most *R. solanacearum*
422 secretion systems. However, expression of the T3SS showed the opposite trend,
423 indicating the specificity of NO-dependent T3SS regulation.

424 When denitrification mutants grew *in planta* they had far fewer alterations in gene
425 expression relative to wild type than when the mutants grew in culture. This suggests
426 that inputs from the plant host help *R. solanacearum* control its metabolism and
427 behaviors. Overall, the cells grown *in planta* seem to encounter less nitrosative stress

428 than cells grown in denitrifying conditions in culture. This could mean that NO stress is
429 not as important *in planta* than in culture, but it does not take into account differences in
430 the microenvironments of the xylem environment. Bacteria grown in culture experience
431 a uniform environment with consistent NO stress. In contrast, *R. solanacearum* cells
432 colonizing plant stems occupy multiple different microenvironments, which likely contain
433 varying NO levels.

434 A previous study compared gene expression between *R. solanacearum* grown in
435 rich media and *R. solanacearum* living in tomato xylem (Jacobs et al. 2012). Although
436 there were methodological differences between that experiment and this one, we saw
437 many similarities in the DEGs present between in culture and *in planta R.*
438 *solanacearum*. In both experiments, many of the most highly upregulated genes are
439 involved in the T3SS. Of the genes that were upregulated *in planta* in both experiments,
440 31 out of 141 (~22%) encoded structural components, regulators, or effectors of the
441 T3SS. Three exceptions to this trend were *prhKLM*. Mutating any of these genes leads
442 to a loss of T3SS gene expression, yet all three were highly downregulated *in planta*
443 compared to either CPG or VDM (Supplementary Table 4) (Zhang et al. 2011; Jacobs et
444 al. 2012). Several other genes that were highly upregulated *in planta* in both
445 experiments encode metabolism of sucrose or myo-inositol, two carbon sources
446 important for *R. solanacearum* during infection (Lowe-Power et al. 2018b; Hamilton et
447 al. 2020; Xian et al. 2020). Additionally, genes involved in flagellar motility were
448 upregulated in both experiments. A similar number of genes (137) were downregulated
449 *in planta* in both experiments. These included several genes predicted to be involved in

450 amino acid transport and metabolism and the superoxide dismutase genes *sodB* and
451 *sodC*.
452 Components of the denitrification pathway were among the most highly
453 upregulated *R. solanacearum* genes *in planta* compared to in rich medium. Consistent
454 with this observation, *R. solanacearum* mutants unable to denitrify were reduced in
455 growth *in planta* and in bacterial wilt virulence (Dalsing et al. 2015). However, the same
456 genes were around 20-fold more highly expressed in denitrifying culture than *in planta*.
457 Further, the RNS-responsive NO-detoxifying genes *norB* and *hmpX* were upregulated *in*
458 *planta* compared to rich media but were expresses much less *in planta* than in
459 denitrifying conditions in culture. This indicates that *Rs* experiences more nitrosative
460 stress when growing in denitrifying culture conditions than when growing in the plant
461 host, which in turn is more nitrosatively stressful than aerobic growth in rich media.
462 These data add to the strong evidence that *R. solanacearum* gene expression and
463 metabolism are very different in the biologically realistic host environment than in
464 culture. This may be due to the complex structure of the xylem environment, where host
465 inputs modulate *R. solanacearum* gene expression, the ability to form defensive biofilms
466 and multiple microenvironments with different nutrient or oxygen concentrations, or
467 because the xylem is a flowing environment, constantly bringing new nutrients into the
468 bacterial habitat. The bacterium's behavior in culture should be regarded as artifactual
469 unless proven otherwise.
470 We attempted to directly measure the concentrations of NO in healthy and
471 infected tomato xylem collected from fluid pooling on a cut stem using the NO-reactive

472 fluorescent dye DAF-FM, electro paramagnetic resonance (EPR), and an NO-sensitive
473 microsensor (Namin et al. 2013; Kleschyov et al. 2007; Yoshioka et al. 1996; Schreiber
474 et al. 2008). While a fluorescent signal was observed when DAF-FM was added to
475 xylem sap, no signal was detected through EPR using the NO spin trap cPTIO or with
476 the microsensor (Unisense, Aarhus, Denmark), suggesting that the DAF-FM
477 fluorescence was not specific to NO. These results highlight the need to measure NO
478 using multiple methods in biological systems (Gupta and Igamberdiev 2013). This
479 failure to detect NO in tomato xylem may not reflect true levels of NO in an intact plant.
480 We collected xylem sap by de-topping tomato plants just above the cotyledons and
481 allowing root pressure to force xylem fluid to pool on the cut stem. Any material exuded
482 in the first two minutes after cutting was removed in an attempt to limit the amount of
483 cellular debris and phloem in the collected material. This method, while useful for
484 obtaining sap to analyze for stable metabolites may not work with a transient metabolite
485 like NO (Lowe-Power et al. 2018a). Cutting the stems stimulates production of reactive
486 oxygen species, which quickly react with NO to form other reactive nitrogen species,
487 potentially diluting any NO signal (Milling et al. 2011; Beckman and Koppenol 1996; Van
488 Faassen and Vanin 2007). Furthermore, this approach can only measure NO levels in
489 bulk xylem sap. The xylem is a dynamic and physically heterogenous environment.
490 Xylem flow, xylem structure, and *R. solanacearum*-produced biofilms may all create
491 gradients or microenvironments with altered NO concentrations in the xylem of intact
492 plants (Zimmermann, 1983; Kim *et al.*, 2016; Tran *et al.*, 2016; Lowe-Power, Khokhani
493 and Allen, 2018). These factors complicate direct measurement of xylem NO. Confocal

494 microscopy of intact infected stems using fluorescent markers to visualize *R.*
495 *solanacearum*, biofilms, and NO may eventually give a more complete understanding of
496 this challenging landscape.

497 Overall, these results reveal a strong connection between NO levels and
498 expression of the *R. solanacearum* T3SS. They suggest that *R. solanacearum* regulates
499 virulence in part by using denitrifying metabolism and the resulting NO as a signal of the
500 hypoxic high-nitrogen host xylem environment. Ongoing work is exploring how *R.*
501 *solanacearum* manages nitrosative stress and identify additional effects of NO on
502 biology of both host plant and bacterial pathogen.

503

504 **Materials and Methods**

505

506 **Bacterial strains and culture conditions.**

507 All strains, plasmids, and primers used in this study are listed in Supplementary
508 Table 1. *R. solanacearum* was cultured in either CPG or a modified VDM medium at
509 28˚C (Hendrick and Sequeira 1984; Dalsing et al. 2015). *E. coli* was grown in Luria-
510 Bertani (LB) media at 37˚C. As needed, cultures were supplemented with antibiotics: 25
511 μg/mL kanamycin or 15 μg/mL gentamicin.

512

513

514 **Strain construction.**

515 An *R. solanacearum* GMI1000 mutant lacking *hrpB* (RSp0873) was created
516 using a modified *sacB*-dependent positive selection vector, pUFR80 (Castañeda et al.
517 2005). The regions directly upstream and downstream of *hrpB* were amplified using the
518 ΔhrpBup/dwn primer pairs. These fragments were then inserted into pUFR80 digested
519 with *Hind*III using Gibson assembly (Sievers et al. 2011). The resulting plasmid,
520 pUFR80-ΔhrpB was transformed into *R. solanacearum* GMI1000 and successful
521 plasmid integrations were selected for kanamycin resistance. The resulting colonies
522 were then counter selected on CPG + 5% w/v sucrose. Successful deletions were
523 confirmed using PCR, sequencing, and a functional screen for the ability to induce HR
524 on the incompatible host *N. tabacum* (Poueymiro et al. 2009).
525 The *ΔhrpB* mutation was complemented by inserting a DNA fragment encoding
526 *hrpB* and *hrcC* with the ~600 bp upstream containing their native promoter into the
527 selectively neutral *att* site in the *R. solanacearum* chromosome using pRCK (Monteiro
528 et al. 2012b). The fragment was amplified using hrpBcomp_F/R and inserted into
529 *AvrII/XbaI*-digested pRCK using Gibson assembly. This vector was then transformed
530 into *ΔhrpB* and selected on CPG+kan.
531
532 **Plant growth conditions.**
533 Wilt-susceptible tomato cv. Bonny Best were germinated and grown in BM2 all-
534 purpose germination and propagation mix (Berger, Saint-Modeste, QC). Plants were
535 grown at 28˚C with a 12 hr photoperiod. Seedlings were transplanted after 14 days.
536 After transplanting, plants were watered on alternate days with 1/2 strength Hoagland

537 solution. Tomato seeds for axenic seedling production were sterilized by washing with
538 10% bleach for ten minutes, followed by two five-minute washes in 70% ethanol, then
539 rinsed five times with water and germinated on water agar plates.
540
541 **Lux reporter assays.**
542 To test the effect of denitrification on T3SS gene expression, *R. solanacearum*
543 strain GMI1000 carrying a *hrpB::lux* reporter gene fusion was grown in denitrifying
544 conditions as follows (Monteiro et al. 2012a). Overnight cultures grown in CPG were
545 resuspended in VDM with or without 30 mM potassium nitrate to an initial OD_{600} of
546 0.001. These cultures were grown in 200 μL volumes in clear-bottomed white-walled 96
547 well plates at 28˚C in 0.1% O_2 with shaking. Every half hour, the Abs_{600} and
548 luminescence was measured using a BioTek SynergyHT microplate reader (BioTek,
549 Winooski, VT, USA). To determine the effects of the NO scavenger cPTIO on T3SS
550 gene expression, *hrpB::lux* cultures were resuspended in 24-well plates in 1 mL of
551 water, either with or without two five day-old sterile tomato seedlings. As appropriate,
552 cPTIO was added to a final concentration of 1 mM. The plates were incubated at 28˚C
553 with shaking for ~24 hours. The pigmented liquid was removed from the seedlings and
554 transferred to 1.5 mL Eppendorf tubes, after which the bacteria were pelleted by
555 centrifugation. The pigmented supernatant was removed, and the pellets resuspended
556 in 200 μL of water. These suspensions were transferred to a new plate and the Abs_{600}
557 and luminescence was measured as detailed above.
558

559 **RNA extraction for sequencing**.

560 To profile gene expression of *R. solanacearum* at various levels of NO stress, we
561 extracted RNA from *R. solanacearum* grown in culture and *in planta*. For each in
562 condition, we used *R. solanacearum* from three separate overnight cultures as
563 biological replicates. For the *in vitro* samples, overnight cultures grown in CPG were
564 resuspended to a final OD_{600} of 0.01 in 50 mL of VDM + 30 mM potassium nitrate in
565 conical tubes. These cultures were incubated without shaking for 12 hours at 28˚C in
566 0.1% O_2. Four hours before harvesting, CysNO or H_2O_2 were added to the relevant
567 cultures to a final concentration of 1 mM and 100 μM, respectively. CysNO was
568 synthesized by adding HCl to a solution containing 200 mM L-cysteine and 200 mM
569 sodium nitrite. The solution was incubated in the dark for ten minutes before it was
570 neutralized by adding sodium hydroxide to a final concentration of 200 mM. The
571 molarity of the solution was determined using the absorbance at 334 nm and the
572 extinction coefficient 90/M*cm. After 16h total incubation, sub-samples were collected
573 for dilution plating to determine CFU/ml and the tubes were capped and centrifuged at
574 room temperature for 5 min at 8000 rpm. The supernatant was removed and pellets
575 were frozen in liquid nitrogen. RNA extractions were carried out using a modified
576 version of the Quick-RNA™ MiniPrep kit (Zymo Research, Irvine, CA, USA), as follows.
577 Pellets were resuspended in 400 μL of ice cold TE pH 8 with 1 mg/mL lysozyme, 0.25
578 μL Superase Inhibitor (Ambion, Austin, TX, USA), and 80 μL of 10% SDS, vortexed for
579 10s, transferred to a new 2 mL tube, and shaken at ~300 rpm for 2 min. 800 μL of RNA-
580 Lysis lysis buffer was added, the tubes were vortexed again for 10 s, cleaned according

581 to the kit manufacturer's instructions, and eluted in 100 μL of water. Nucleic acid
582 concentrations were estimated using a nanodrop, normalized to 200 ng/uL, and cleaned
583 using the DNA-free DNAse kit (Invitrogen, Carlsbad, CA, USA). Samples were
584 incubated at 37C for 1 hour, with 2 μL more of DNAse added at 30 min. After DNAse
585 inactivation, samples were further cleaned by chloroform extraction, then precipitated
586 overnight at -20˚C with 100 μM Sodium Acetate pH 5.5 and 66 % ethanol. Samples
587 were checked for concentration on a Nanodrop, for DNA contamination by PCR using
588 the qRT-PCR primers *serC*_F/R, and for RNA integrity (RIN) using an Agilent
589 Bioanalyzer 21000 (Agilent, Santa Clara, CA, USA). All samples had RIN values above
590 7.3.

591 The *in planta* samples were harvested after 21 day old Bonny Best tomatoes
592 were inoculated with ~2000 CFU of each bacteria strain through the cut petiole of the
593 first true leaf. At 3 dpi, approximately 0.1 g of stem tissue was collected from the site of
594 inoculation, immediately frozen in liquid nitrogen, and stored at -80˚C. Another ~0.1 g of
595 tissue was collected from directly below the inoculation site and was ground in bead
596 beater tubes using a PowerLyzer (Qiagen, Hilden, Germany) for two cycles of 2200 rpm
597 for 90 s in each with a 4 min rest between cycles. This material was then dilution plated
598 to measure bacterial colonization. From each biological replicate, we chose six plants
599 with the most similar level of colonization. RNA was extracted from these using a
600 modified hot phenol-chloroform method (Jacobs et al. 2012). Between 4 and 5 individual
601 plants were pooled per biological replicate. Nucleic acid sample quality was checked

602 using a nanodrop, Agilent bioanalyzer, and qRT-PCR primers Actin_F/R. All samples
603 had RIN values of above 7.2.
604
605 **RNA sequencing and data analysis.**
606 All RNA was sent to Novogene (Beijing, China) for library preparation,
607 sequencing, and analysis. rRNA depletion, fragmentation, and library construction were
608 done using NEBNext® *μ*Ltra™ Directional RNA Library Prep Kit for Illumina® (NEB,
609 Ipswitch, MA, USA) following the manufacturer's recommendation and starting with 3 μg
610 of RNA per sample. After the libraries were constructed, their quality was assessed
611 using an Agilent Bioanalyzer 21000 system and sequenced using an Illumina platform
612 to generate paired-end reads. Between 19,000,000 and 40,000,000 reads were
613 produced per sample. Raw reads were converted to FASTQ files using Illumina
614 CASAVA v1.8, and then filtered for quality, removing reads with adaptor contamination,
615 greater than 10% uncertain nucleotides, or more than 50% of nucleotides with a Q_{pred}
616 less than or equal to 5. Over 95% of reads were of good quality, and were mapped to
617 the *R. solanacearum* GMI1000 genome
618 (https://www.ncbi.nlm.nih.gov/assembly/GCF_000009125.1) using Bowtie2 -2.2.3
619 (Langmead et al. 2009). From this, gene expression was calculated using HTseq v0.6.1
620 and differential gene expression was calculated using DESeq 1.18.0. P-values
621 calculated by DESeq were adjusted to control for the false discovery rate (FDR) using
622 the Benjamini-Hochberg approach. Gene Ontology enrichment was analyzed using

623 GOseq Release2.12 and KEGG enrichment was calculated using KOBAS v2.0
624 software.
625
626 **Measuring T3SS expression with qRT-PCR.**
627 Expression of T3SS genes was measured in denitrification mutants grown in 40
628 mL of VDM + 30 mM nitrate grown in GasPak™ EZ microaerobic pouches (BD, Franklin
629 Lakes, NJ, USA) at 28˚C with shaking for 18 hours starting from an OD_{600} of 0.001.
630 RNA extractions were carried out using a hot phenol-chloroform method (Jacobs et al.
631 2012). Extractions were carried out using the Quick-RNA™ MiniPrep kit (Zymo
632 Research, Irvine, CA, USA). cDNA synthesis was done using the Superscript VILO
633 cDNA synthesis kit (Invitrogen, Carlsbad, CA, USA). qPCR reactions were carried out in
634 10 μL volumes using 5 ng of total template using PowerUp Syber Green Master) in a
635 QuantStudio 5 Real-Time PCR System Mix (Applied Biosystems, Foster City, CA,
636 USA).
637
638 **Data Availability**
639 The data supporting this research are openly available in the Gene Expression
640 Omnibus at https://www.ncbi.nlm.nih.gov/geo/query/acc.cgi?acc=GSE160024, GEO
641 accession: GSE160024.
642
643 **Acknowledgments**

The authors would like to thank Jon Jacobs for discussion and advice throughout the project and Max Miao for his expertise and discussion about statistics and R. CGH and BLD were supported by NSF predoctoral fellowships. This material is based upon work supported by the National Science Foundation Graduate Research Fellowship Program under Grant No. DGE-1747503. Any opinions, findings, and conclusions or recommendations expressed in this material are those of the author(s) and do not necessarily reflect the views of the National Science Foundation. The authors declare no competing financial interests

References

Aldon, D., Brito, B., Boucher, C., and Genin, S. 2000. A bacterial sensor of plant cell contact controls the transcriptional induction of *Ralstonia solanacearum* pathogenicity genes. Embo J. 19:2304–2314

Arlat, M., Gough, C. L., Zischek, C., Barberis, P. a, Trigalet, A., and Boucher, C. a. 1992. Transcriptional organization and expression of the large hrp gene cluster of *Pseudomonas solanacearum*. Mol. Plant. Microbe. Interact. 5:187–193

Asgher, M., Per, T. S., Masood, A., Fatma, M., Freschi, L., Corpas, F. J., and Khan, N. A. 2017. Nitric oxide signaling and its crosstalk with other plant growth regulators in plant responses to abiotic stress. Environ. Sci. Pollut. Res. 24:2273–2285

Astuti, R. I., Nasuno, R., and Takagi, H. 2018. Nitric Oxide Signalling in Yeast. Adv. Microb. Physiol. 72:29–63

Beckman, J. S., and Koppenol, W. H. 1996. Nitric oxide, superoxide, and peroxynitrite: the good, the bad, and ugly. Am. J. Physiol. 271:C1424-37

Boucher, C. A., Barberis, P. A., Trigalet, A. P., and Demery, D. A. 1985. Transposon mutagenesis of *Pseudomonas solanacearum*: Isolation of Tn5-induced avirulent mutants. J. Gen. Microbiol. 131:2449–2457

Brito, B., Marenda, M., and Barberis, P. 1999. *prhJ* and *hrpG*, two new components of

672 the plant signal-dependent regulatory cascade controlled by PrhA in *Ralstonia*
673 *solanacearum*. Mol. Microbiol. 31:237–251

674 Carlson, H. K., Vance, R. E., and Marletta, M. A. 2010. H-NOX Regulation of c-di-GMP
675 Metabolism and Biofilm Formation in *Legionella pneumophila*. Mol. Microbiol.
676 77:930–942

677 Castañeda, A., Reddy, J., El-Yacoubi, B., and Gabriel, D. 2005. Mutagenesis of all eight
678 *avr* genes in *Xanthomonas campestris* pv. *campestris* had no detected effect on
679 pathogenicity, but one *avr* gene affected race specificity. Mol. Plant-Microbe
680 Interact. 18:1306–1317

681 Cooper, C. E. 1999. Nitric oxide and iron proteins. Biochim. Biophys. Acta - Bioenerg.
682 1411:290–309

683 Cunnac, S., Occhialini, A., Barberis, P., Boucher, C., and Genin, S. 2004. Inventory and
684 functional analysis of the large Hrp regulon in *Ralstonia solanacearum*:
685 identification of novel effector proteins translocated to plant host cells through the
686 type III secretion system. Mol. Microbiol. 53:115–128

687 D'Alessandro, S., Posocco, B., Costa, A., Zahariou, G., Schiavo, F. Lo, Carbonera, D.,
688 and Zottini, M. 2013. Limits in the use of cPTIO as nitric oxide scavenger and EPR
689 probe in plant cells and seedlings. Front. Plant Sci. 4:340

690 Dalsing, B. L., Truchon, A. N., Gonzalez-Orta, E. T., Milling, A. S., and Allen, C. 2015.
691 *Ralstonia solanacearum* uses inorganic nitrogen metabolism for virulence, ATP
692 production, and detoxification in the oxygen-limited host xylem environment. MBio.
693 6:1–13

694 Delledonne, M., Xia, Y., Dixon, R. a, and Lamb, C. 1998. Nitric oxide functions as a
695 signal in plant disease resistance. Nature. 394:585–588

696 Elphinstone, J. 2005. The current bacterial wilt situation: a global overview. Pages 9–28
697 in: Bacterial Wilt: The Disease and the *Ralstonia solanacearum* Species Complex.,
698 C. Allen, P. Prior, and A.C. Hayward, eds. Society, American Phytopathological, St
699 Paul, MN.

700 Van Faassen, E., and Vanin, A. F. 2007. *Nitric oxide radicals and their reactions*.
701 Elsevier B.V.

702 Farr, S. B., and Kogoma, T. 1991. Oxidative stress responses in *Escherichia coli* and
703 *Salmonella typhimurium*. Microbiol. Rev. 55:561–585

704 Ge, S. X., Son, E. W., and Yao, R. 2018. iDEP: An integrated web application for
705 differential expression and pathway analysis of RNA-Seq data. BMC
706 Bioinformatics. 19:1–24

707 Génin, S., Brito, B., Denny, T. P., and Boucher, C. 2005. Control of the *Ralstonia*
708 *solanacearum* Type III secretion system (Hrp) genes by the global virulence
709 regulator PhcA. FEBS Lett. 579:2077–2081

710 Genin, S., and Denny, T. P. 2012. Pathogenomics of the *Ralstonia solanacearum*
711 species complex. Annu. Rev. Phytopathol. 50:67–89

712 Genin, S., Gough, C. L., Zischek, C., and Boucher, C. A. 1992. Evidence that the *hrpB*
713 gene encodes a positive regulator of pathogenicity genes from *Pseudomonas*
714 *solanacearum*. Mol. Microbiol. 6:3065–3076

715 Van Gijsegem, F., Gough, C., Zischek, C., Niqueux, E., Arlat, M., Genin, S., Barberis,
716 P., German, S., Castello, P., and Boucher, C. 1995. The hrp gene locus of
717 *Pseudomonas solanacearum*, which controls the production of a type III secretion
718 system, encodes eight proteins related to components of the bacterial flagellar
719 biogenesis complex. Mol. Microbiol. 15:1095–1114

720 Gupta, K. J., and Igamberdiev, A. U. 2013. Recommendations of using at least two
721 different methods for measuring NO. Front. Plant Sci. 4:2–5

722 Hamilton, C. D., Steidl, O. R., Macintyre, A. M., Hendrich, C. G., and Allen, C. 2020.
723 *Ralstonia solanacearum* depends on catabolism of myo-inositol, sucrose, and
724 trehalose for virulence in an infection stage-dependent manner. MPMI.

725 Hanahan, D. 1983. Studies on Transformation of *Escherichia coli* with Plasmids. J. Mol.
726 Biol. 166:557–580

727 Henares, B. M., Higgins, K. E., and Boon, E. M. 2012. Discovery of a Nitric Oxide
728 Responsive Quorum Sensing Circuit in *Vibrio harveyi*. ACS Chem. Biol. 7:1331–
729 1336

730 Hendrick, C. A., and Sequeira, L. 1984. Lipopolysaccharide-defective mutants of the wilt
731 pathogen *Pseudomonas solanacearum*. Appl. Environ. Microbiol. 48:94–101

732 Hossain, S., and Boon, E. M. 2017. Discovery of a Novel Nitric Oxide Binding Protein
733 and Nitric-Oxide- Responsive Signaling Pathway in *Pseudomonas aeruginosa*.
734 ACS Infect. Dis. 3:454–461

735 Husain, M., Jones-carson, J., Song, M., Mccollister, B. D., and Bourret, T. J. 2010.
736 Redox sensor SsrB Cys 203 enhances *Salmonella* fitness against nitric oxide
737 generated in the host immune response to oral infection. Proc Natl Acad Sci U S A.
738 107:4–13

739 Jacobs, J. M., Babujee, L., Meng, F., Milling, A. S., and Allen, C. 2012. The *in planta*
740 transcriptome of *Ralstonia solanacearum*: conserved physiological and virulence
741 strategies during bacterial wilt of tomato. MBio. 3:e00114-12

742 Khokhani, D., Lowe-Power, T. M., Tran, T. M., and Allen, C. 2017. A Single Regulator
743 Mediates Strategic Switching between Attachment / Spread and Growth / Virulence
744 in the Plant Pathogen *Ralstonia solanacearum*. MBio. 8:1–20

745 Kim, M. K., Ingremeau, F., Zhao, A., Bassler, B. L., and Stone, H. A. 2016. Local and
746 global consequences of flow on bacterial quorum sensing. Nat. Microbiol. 1:15005

747 Kleschyov, A. L., Wenzel, P., and Munzel, T. 2007. Electron paramagnetic resonance
748 (EPR) spin trapping of biological nitric oxide. J. Chromatogr. B Anal. Technol.
749 Biomed. Life Sci.

750 Kolbert, Z., Feigl, G., Bordé, Á., Molnár, Á., and Erdei, L. 2017. Protein tyrosine nitration
751 in plants: Present knowledge, computational prediction and future perspectives.
752 Plant Physiol. Biochem. 113:56–63

753 Langmead, B., Trapnell, C., Pop, M., and Salzberg, S. L. 2009. Ultrafast and memory-
754 efficient alignment of short DNA sequences to the human genome. Genome Biol.
755 10

756 Leitner, M., Vandelle, E., Gaupels, F., Bellin, D., and Delledonne, M. 2009. NO signals
757 in the haze. Nitric oxide signalling in plant defence. Curr. Opin. Plant Biol. 12:451–
758 458

759 Liu, N., Xu, Y., Hossain, S., Huang, N., Coursolle, D., and Gralnick, J. A. 2012. Nitric
760 Oxide Regulation of Cyclic di-GMP Synthesis and Hydrolysis in *Shewanella*
761 *woodyi*. Biochemistry. 51:2087–2099

762 Liu, Z., Cao, J., Ma, Q., Gao, X., Ren, J., and Xue, Y. 2011. GPS-YNO2: computational
763 prediction of tyrosine nitration sites in proteins. Mol. Biosyst. 7:1197

764 Lonjon, F., Lohou, D., Cazalé, A. C., Büttner, D., Ribeiro, B. G., Péanne, C., Genin, S.,
765 and Vailleau, F. 2017. HpaB-Dependent Secretion of Type III Effectors in the Plant
766 Pathogens *Ralstonia solanacearum* and *Xanthomonas campestris* pv. *vesicatoria*.
767 Sci. Rep. 7:1–14

768 Lonjon, F., Turner, M., Henry, C., Rengel, D., Lohou, D., van de Kerkhove, Q., Cazale,
769 A.-C., Peeters, N., Genin, S., and Vailleau, F. 2015. Comparative Secretome
770 Analysis of *Ralstonia solanacearum* Type 3 Secretion-Associated Mutants Reveals
771 a Fine Control of Effector Delivery, Essential for Bacterial Pathogenicity. Mol. Cell.
772 Proteomics.

773 Lowe-Power, T. M., Hendrich, C. G., von Roepenack-Lahaye, E., Li, B., Wu, D., Mitra,
774 R., Dalsing, B. L., Ricca, P., Naidoo, J., Cook, D., Jancewicz, A., Masson, P.,
775 Thomma, B., Lahaye, T., Michael, A. J., and Allen, C. 2018a. Metabolomics of
776 tomato xylem sap during bacterial wilt reveals *Ralstonia solanacearum* produces
777 abundant putrescine, a metabolite that accelerates wilt disease. Environ. Microbiol.

778 20:1330–1349

779 Lowe-Power, T. M., Khokhani, D., and Allen, C. 2018b. How *Ralstonia solanacearum*
780 Exploits and Thrives in the Flowing Plant Xylem Environment. Trends Microbiol.
781 26:929–942

782 Marc Marenda, Callard, B. B. D., Genin, S., Barberis, P., Boucher, C., and Arlat, M.
783 1998. PrhA controls a novel regulatory pathway required for the specific induction
784 of *Ralstonia solanacearum hrp* genes in the presence of plant cells. Mol. Microbiol.
785 27:437–453

786 Milling, A. S., Babujee, L., and Allen, C. 2011. *Ralstonia solanacearum* extracellular
787 polysaccharide is a specific elicitor of defense responses in wilt-resistant tomato
788 plants. PLoS One. 6

789 Monteiro, F., Genin, S., van Dijk, I., and Valls, M. 2012a. A luminescent reporter
790 evidences active expression of *Ralstonia solanacearum* type III secretion system
791 genes throughout plant infection. Microbiol. (United Kingdom). 158:2107–2116

792 Monteiro, F., Solé, M., van Dijk, I., and Valls, M. 2012b. A chromosomal insertion
793 toolbox for promoter probing, mutant complementation, and pathogenicity studies in
794 *Ralstonia solanacearum*. Mol. Plant. Microbe. Interact. 25:557–68

795 Namin, S. M., Nofallah, S., Joshi, M. S., Kavallieratos, K., and Tsoukias, N. M. 2013.
796 Kinetic analysis of DAF-FM activation by NO: Toward calibration of a NO-sensitive
797 fluorescent dye. Nitric Oxide - Biol. Chem. 28:39–46

798 Network, C. S., Plate, L., and Marletta, M. A. 2012. Article Nitric Oxide Modulates
799 Bacterial Biofilm Formation through a Multicomponent. Mol. Cell. 46:449–460

800 Oksanen, J., Blanchet, G., Friendly, M., Kindt, R., Legendre, P., McGlinn, D., Minchin,
801 P. R., O'Hara, R. B., Simpson, G. L., Solymos, P., Stevens, M. H. H., Szoecs, E.,
802 and Wagner, H. 2019. vegan: Community Ecology Package. R package version
803 2.5-6. Available at: https://cran.r-project.org/package=vegan.

804 Peeters, N., Carrère, S., Anisimova, M., Plener, L., Cazalé, A.-C., and Genin, S. 2013.
805 Repertoire, unified nomenclature and evolution of the Type III effector gene set in
806 the *Ralstonia solanacearum* species complex. BMC Genomics. 14:859

807 Perrier, A., Barlet, X., Peyraud, R., Rengel, D., Guidot, A., and Genin, S. 2018.
808 Comparative transcriptomic studies identify specific expression patterns of
809 virulence factors under the control of the master regulator PhcA in the *Ralstonia*
810 *solanacearum* species complex. Microb. Pathog. 116:273–278

811 Peyraud, R., Cottret, L., Marmiesse, L., and Genin, S. 2018. Control of primary
812 metabolism by a virulence regulatory network promotes robustness in a plant

813 pathogen. Nat. Commun. 9:418

814 Pfeiffer, S., Leopold, E., Hemmens, B., Schmidt, K., Werner, E. R., and Mayer, B. 1997.
815 Interference of carboxy-PTIO with nitric oxide-and peroxynitrite- mediated
816 reactions. Free Radic. Biol. Med. 22:787–794

817 Plener, L., Manfredi, P., Valls, M., and Genin, S. 2010. PrhG, a transcriptional regulator
818 responding to growth conditions, is involved in the control of the type III secretion
819 system regulon in *Ralstonia solanacearum*. J. Bacteriol. 192:1011–1019

820 Poueymiro, M., Cunnac, S., Barberis, P., Deslandes, L., Peeters, N., Cazale-Noel, A.-
821 C., Boucher, C., and Genin, S. 2009. Two Type III Secretion System Effectors from
822 *Ralstonia solanacearum* GMI1000 Determine Host-Range Specificity on Tobacco.
823 Mol. Plant-Microbe Interact. 22:538–550

824 Poueymiro, M., and Genin, S. 2009. Secreted proteins from *Ralstonia solanacearum*: a
825 hundred tricks to kill a plant. Curr. Opin. Microbiol. 12:44–52

826 Rao, M., Smith, B. C., and Marletta, M. A. 2015. Nitric Oxide mediates biofilm formation
827 and symbiosis in *Silicibacter* sp. strain TrichCH4B. MBio. 6:1–10

828 Rhee, K. Y., Erdjument-Bromage, H., Tempst, P., and Nathan, C. F. 2005. S-nitroso
829 proteome of *Mycobacterium tuberculosis*: Enzymes of intermediary metabolism and
830 antioxidant defense. Proc. Natl. Acad. Sci. U. S. A. 102:467–72

831 Russwurm, M., and Koesling, D. 2004. NO activation of guanylyl cyclase. EMBO J.
832 23:4443–4450

833 Scheler, C., Durner, J., and Astier, J. 2013. Nitric oxide and reactive oxygen species in
834 plant biotic interactions. Curr. Opin. Plant Biol. 16:534–539

835 Schreiber, F., Polerecky, L., and De Beer, D. 2008. Nitric oxide microsensor for high
836 spatial resolution measurements in biofilms and sediments. Anal. Chem. 80:1152–
837 1158

838 Senuma, W., Takemura, C., Hayashi, K., Ishikawa, S., Kiba, A., Ohnishi, K., Kai, K., and
839 Hikichi, Y. 2020. The putative sensor histidine kinase PhcK is required for the full
840 expression of *phcA* encoding the global transcriptional regulator to drive the
841 quorum-sensing circuit of *Ralstonia solanacearum* strain OE1-1. Mol. Plant Pathol.
842 :1–15

843 Seth, D., Hausladen, A., Wang, Y.-J., and Stamler, J. S. 2012. Endogenous Protein S-
844 Nitrosylation in *E. coli*: Regulation by OxyR. Science (80-.). 336:470–3

845 Sievers, F., Wilm, A., Dineen, D., Gibson, T. J., Karplus, K., Li, W., Lopez, R.,
846 McWilliam, H., Remmert, M., Soding, J., Thompson, J. D., and Higgins, D. G. 2011.

847 Fast, scalable generation of high-quality protein multiple sequence alignments
848 using Clustal Omega. Mol. Syst. Biol. 7:539–545

849 Simmonds, M. J., Detterich, J. A., and Connes, P. 2014. Nitric oxide, vasodilation and
850 the red blood cell. Biorheology. 51:121–134

851 Simontacchi, M., Galatro, A., Ramos-Artuso, F., and Santa-María, G. E. 2015. Plant
852 Survival in a Changing Environment: The Role of Nitric Oxide in Plant Responses
853 to Abiotic Stress. Front. Plant Sci. 6:977

854 Swanson, J. K., Montes, L., Mejia, L., and Allen, C. 2007. Detection of latent infections
855 of *Ralstonia solanacearum* race 3 biovar 2 in geranium. Plant Dis. 91:828–834

856 Tran, T., MacIntyre, A., Khokhani, D., Hawes, M. C., and Allen, C. 2016. Extracellular
857 DNases of *Ralstonia solanacearum* modulate biofilms and facilitate bacterial wilt
858 virulence. Environ. Microbiol. Environ. Microbiol. Reports. 00:1–15

859 Vasse, J., Frey, P., and Trigalet, A. 1994. Microscopic studies of intercellular infection
860 and protoxylem invasion of tomato roots by *Pseudomonas solanacearum*. MPMI.
861 8:241–251

862 Wilson, I. D., Neill, S. J., and Hancock, J. T. 2008. Nitric oxide synthesis and signalling
863 in plants. Plant, Cell Environ. 31:622–631

864 Wünsche, H., Baldwin, I. T., and Wu, J. 2011. S-Nitrosoglutathione reductase (GSNOR)
865 mediates the biosynthesis of jasmonic acid and ethylene induced by feeding of the
866 insect herbivore *Manduca sexta* and is important for jasmonate-elicited responses
867 in *Nicotiana attenuata*. J. Exp. Bot. 62:4605–4616

868 Xian, L., Yu, G., Wei, Y., Rufian, J. S., Li, Y., Zhuang, H., Xue, H., Morcillo, R. J. L., and
869 Macho, A. P. 2020. A Bacterial Effector Protein Hijacks Plant Metabolism to
870 Support Pathogen Nutrition. Cell Host Microbe. :1–10

871 Xue, Y., Liu, Z., Gao, X., Jin, C., Wen, L., Yao, X., and Ren, J. 2010. GPS-SNO:
872 Computational prediction of protein s-nitrosylation sites with a modified GPS
873 algorithm. PLoS One. 5:1–7

874 Yoshioka, T., Iwamoto, N., and Ito, K. 1996. An application of electron paramagnetic
875 resonance to evaluate nitric oxide and its quenchers. J. Am. Soc. Nephrol. 7:961–
876 965

877 Yuliar, Nion, Y. A., and Toyota, K. 2015. Recent trends in control methods for bacterial
878 wilt diseases caused by *Ralstonia solanacearum*. Microbes Environ. 30:1–11

879 Zhang, R., Hess, D. T., Qian, Z., Hausladen, A., Fonseca, F., Chaube, R., Reynolds, J.
880 D., and Stamler, J. S. 2015a. Hemoglobin βCys93 is essential for cardiovascular

881 function and integrated response to hypoxia. Proc. Natl. Acad. Sci. U. S. A.
882 112:6425–6430

883 Zhang, Y., Kiba, A., Hikichi, Y., and Ohnishi, K. 2011. prhKLM genes of *Ralstonia*
884 *solanacearum* encode novel activators of hrp regulon and are required for
885 pathogenesis in tomato. FEMS Microbiol. Lett. 317:75–82

886 Zhang, Y., Li, J., Zhang, W., Shi, H., Luo, F., Hikichi, Y., Shi, X., and Ohnishi, K. 2018.
887 A putative LysR-type transcriptional regulator PrhO positively regulates the type III
888 secretion system and contributes to the virulence of *Ralstonia solanacearum*. Mol.
889 Plant Pathol. :1–12

890 Zhang, Y., Luo, F., Wu, D., Hikichi, Y., Kiba, A., Igarashi, Y., Ding, W., and Ohnishi, K.
891 2015b. PrhN, a putative marR family transcriptional regulator, is involved in positive
892 regulation of type III secretion system and full virulence of *Ralstonia solanacearum*.
893 Front. Microbiol. 6:1–12

894 Zimmermann, M. H. 1983. *Xylem Structure and the Ascent of Sap*. Springer-Verlag,
895 Berlin.

896 Zuluaga, A. P., Puigvert, M., and Valls, M. 2013. Novel plant inputs influencing
897 *Ralstonia solanacearum* during infection. Front. Microbiol. 4:1–7

898

899

900 **Supplementary Table 1. Bacterial strains, plasmids, and primers**

Strains	**Relevant characteristics**	**Reference**
R. solanacearum		
GMI1000	Phylotype I seq 18 strain isolated from tomato in French Guyana	(Boucher et al. 1985)
hrpB::lux	GMI1000 expressing the bacterial *lux* reporter controlled by the *hrpB* promoter, Kan^R	(Monteiro et al. 2012a)
ΔnarG	GMI1000 lacking *narG*, a nitrate reductase. Cannot denitrify and does not produce NO, Gm^R	(Dalsing et al. 2015)
ΔnorB	GMI1000 lacking *norB*, a nitric oxide reductase. Can denitrify, but accumulates NO, Gm^R	(Dalsing et al. 2015)
ΔhrpB	GMI1000 lacking *hrpB*. Avirulent and does not express a T3SS	This study
hrpB comp	*ΔhrpB* complemented.,Kan^R	This study
E. coli		
DH5α	dlacZ, Delta M15 Delta(lacZYA-argF) U169 recA1 endA1 hsdR17(rK-mK+) supE44 thi-1 gyrA96 relA1	(Hanahan 1983)
Plasmid	**Description**	**Reference**
pUFR80	Positive sucrose selection vector, Suc^S, Kan^R	(Castañeda et al. 2005)
pRCK-GWY	Gateway destination vector that integrates into the GMI1000 genome at the neutral *att* site; Kan^R	(Monteiro et al. 2012b)
pUFR80-ΔhrpB	Vector used to make unmarked *R. solanacearum ΔripB*, Suc^S, Kan^R	This study
pRCK-hrpBco	Complementation vector containing WT *hrpB* and *hrcC*, Kan^R	This study

mp		
Cloning Primers		
Primer	**Sequence[a]**	**Reference**
ΔhrpBup_F	5' – cgacggccagtgccaGTTCGATACCAGCGAAAGC target locus: RSp0873	This study
ΔhrpBup_R	5' – cggagggcGGCAATGCTCCTGAAGCG target locus: RSp0873	This study
ΔhrpBdwn_F	5' – gcattgccGCCCTCCGGCGGACCGCC target locus: RSp0873	This study
ΔhrpBdwn_R	5' – acctgcaggcatgcaGCTGTTGCCGACGTATTGACCGGTGC target locus: RSp0873	This study
hrpBcomp_F	5' – tgcgcgagcaggggaattgcGACAACGTCTCCGGGTTC target locus: RSp0873-RSp0874	This study
hrpBcomp_R	5' – cgaccctagtctaagatcttCTTCGGCATTCGGCAATG target locus: RSp0873-RSp0874	This study
qRT-PCR Primers		
Primer	**Sequence**	**Reference**
hrpB_F	5' – CCTGCCCGAATACGCAAATG target locus: RSp0873	This study
hrpB_R	5' – CGAATGGCGGATCAGGCGCT target locus: RSp0873	This study
hrpG_F	5' – GCAGAACGTGGAATGTGTCC target locus: R. solanacearump0852	This study
hrpG_R	5' – AGACTGAATGCCTCGGTACG target locus: RSp0852	This study
ripAA_F	5' – GGAATACAGCAACTGCGTGC target locus: RSc0608	This study
ripAA_R	5' – TTGTAGTTGCGGACCCTCAGtarget locus: RSc0608	This study
serC_F	5' – CGCGCAAATACGGTGAAGTG target locus: R. solanacearumc0903	This study
serC_R	5' – GTGCACAGATGCACGTAAGC target locus: RSc0903	This study
Actin_F	5' – TCAGCAACTGGGATGATATG target locus: BT013524	(Milling et al. 2011)

Actin_R	5' – TTAGGGTTGAGAGGTGCTTC target locus: BT013524	(Milling et al. 2011)

901 [a] Capitalized bp anneal to the target locus, non-capitalized bp anneal to other fragments

902 in a Gibson assembly reaction

903

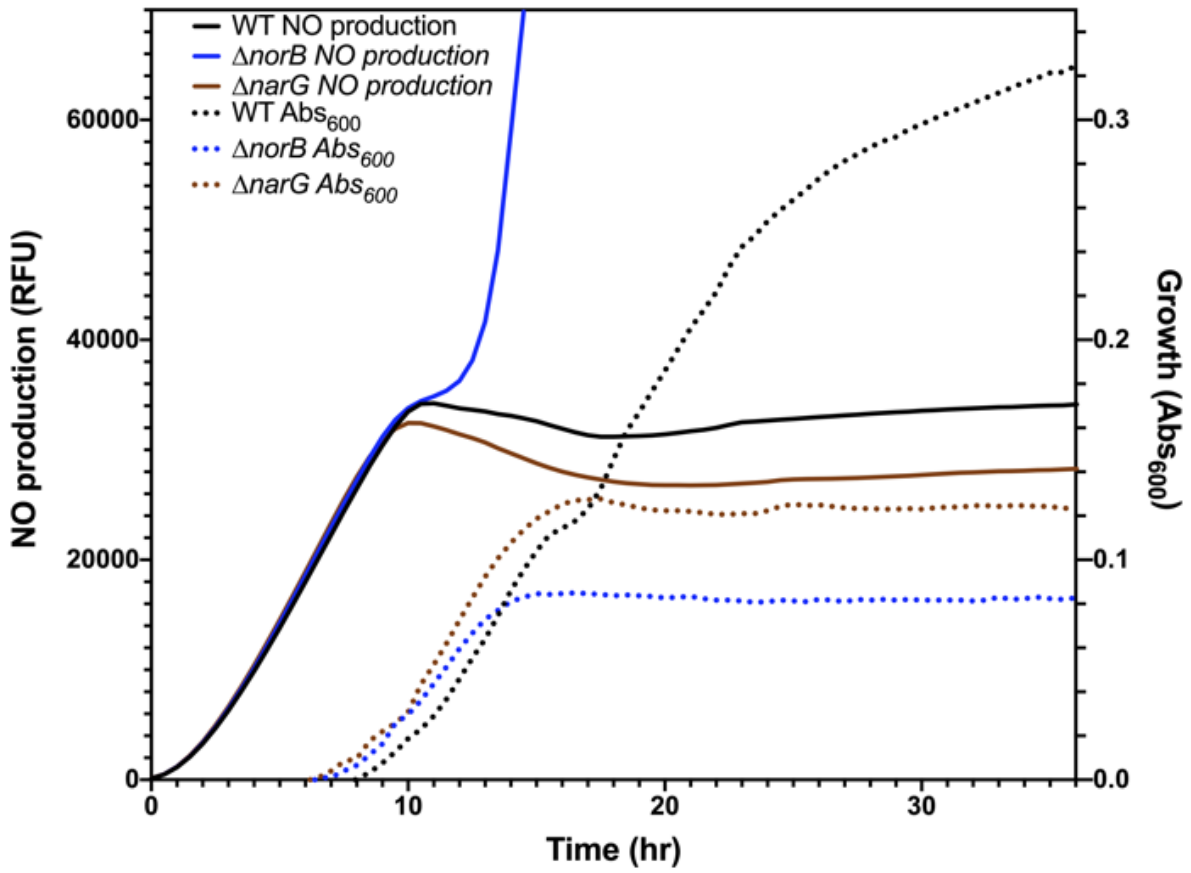

904

905 **Supplementary Fig. 1.** Growth and NO levels of *R. solanacearum* strains under

906 denitrifying conditions in culture. Cultures were started at a concentration of 10^6

907 CFU/mL in VDM containing the NO-detecting fluorescent dye DAF-FM DA at 10 μM.

908 Cultures were incubated in in clear-bottomed, white-walled 96-well plates at 30C for 24

909 h at $[O_2]$ =0.1%. Culture growth (dotted lines) is shown as absorbance at 600 nm. NO

910 concentration (solid lines) was measured as DAF-FM fluorescence at 495/515 nm. The

911 *ΔnorB* mutant strain accumulates NO, which significantly impairs its growth.

912

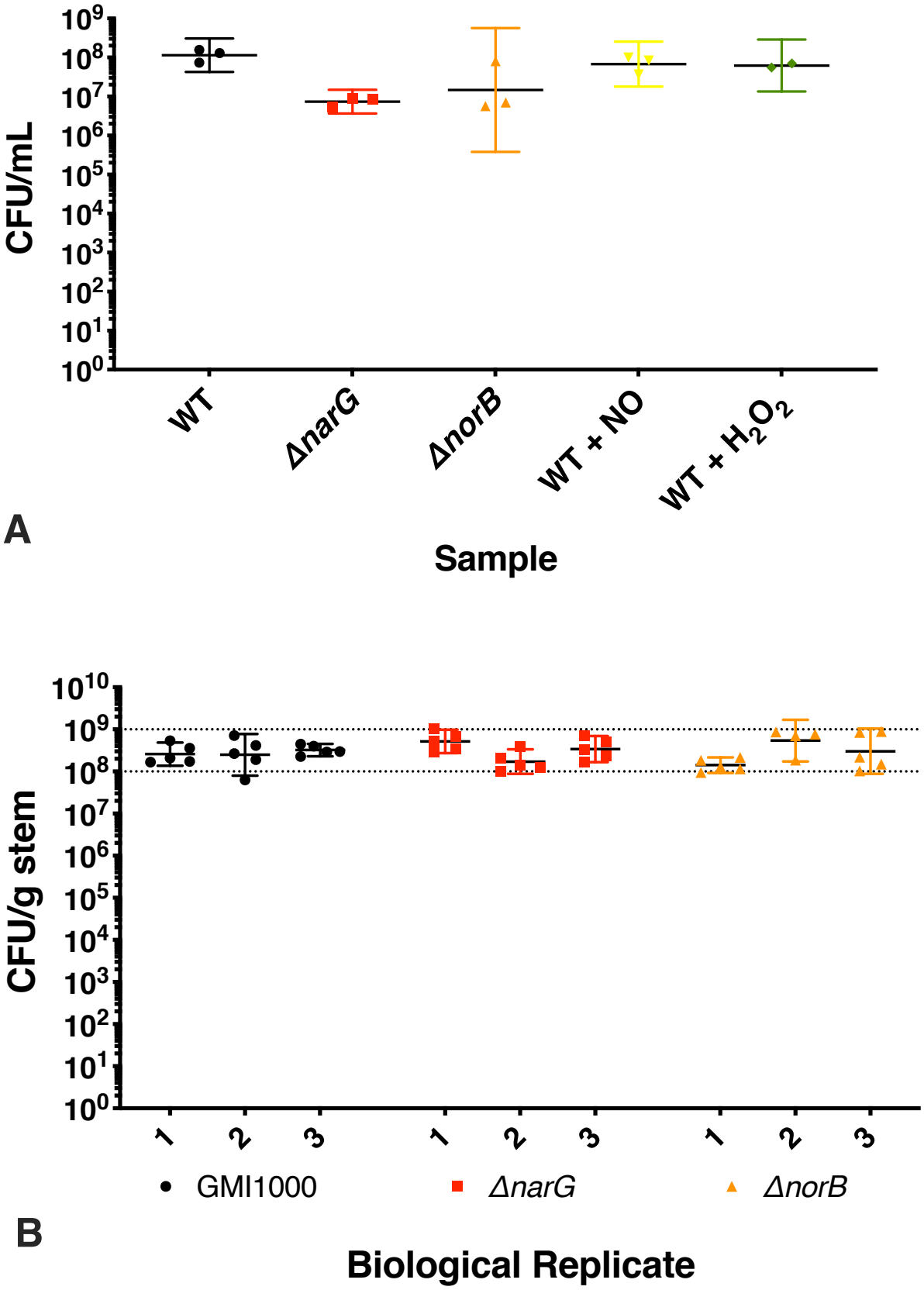
CFU/mL
10^9
10^8
10^7
10^6
10^5
10^4
10^3
10^2
10^1
10^0
WT
ΔnarG
ΔnorB
WT + NO
WT + H_2O_2
A
Sample
CFU/g stem
10^{10}
10^9
10^8
10^7
10^6
10^5
10^4
10^3
10^2
10^1
10^0
1
2
3
1
2
3
1
2
3
GMI1000
ΔnarG
ΔnorB
B
Biological Replicate

913

914 **Supplementary Fig. 2.** In vitro cell densities and tomato stem colonization of samples
915 used in RNA-seq. **A,** Cell densities of culture samples as measured by dilution plating.
916 One H_2O_2-treated plate was uncountable due to plate contamination. OD_{600} values of
917 each culture were also collected and had comparable values. **B,** Colonization of tomato
918 plants used for transcriptome sequencing. Roughly 0.1 g of stem tissue was collected
919 from directly below the sample used for sequencing. The tissue was ground and dilution
920 plated to enumerate CFU/g stem.
921

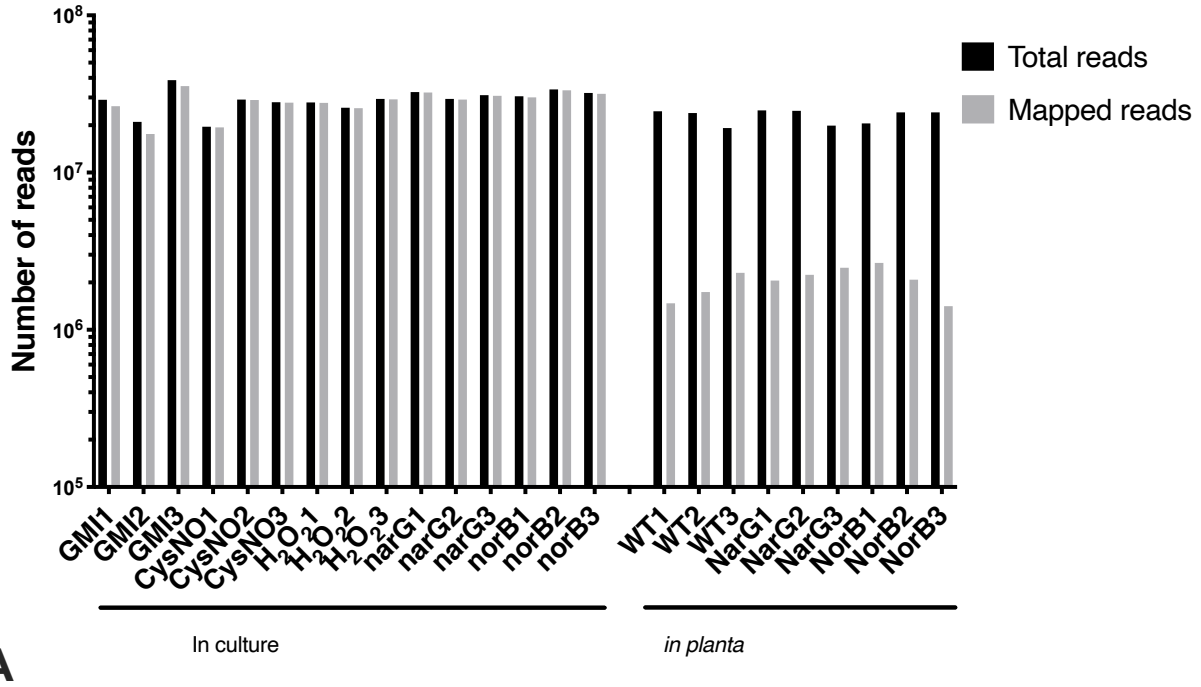
Total reads
Mapped reads
Number of reads
10^8
10^7
10^6
10^5
GMI1
GMI2
GMI3
CysNO1
CysNO2
CysNO3
$H_2O_2$1
$H_2O_2$2
$H_2O_2$3
narG1
narG2
narG3
norB1
norB2
norB3
WT1
WT2
WT3
NarG1
NarG2
NarG3
NorB1
NorB2
NorB3
In culture
in planta
A

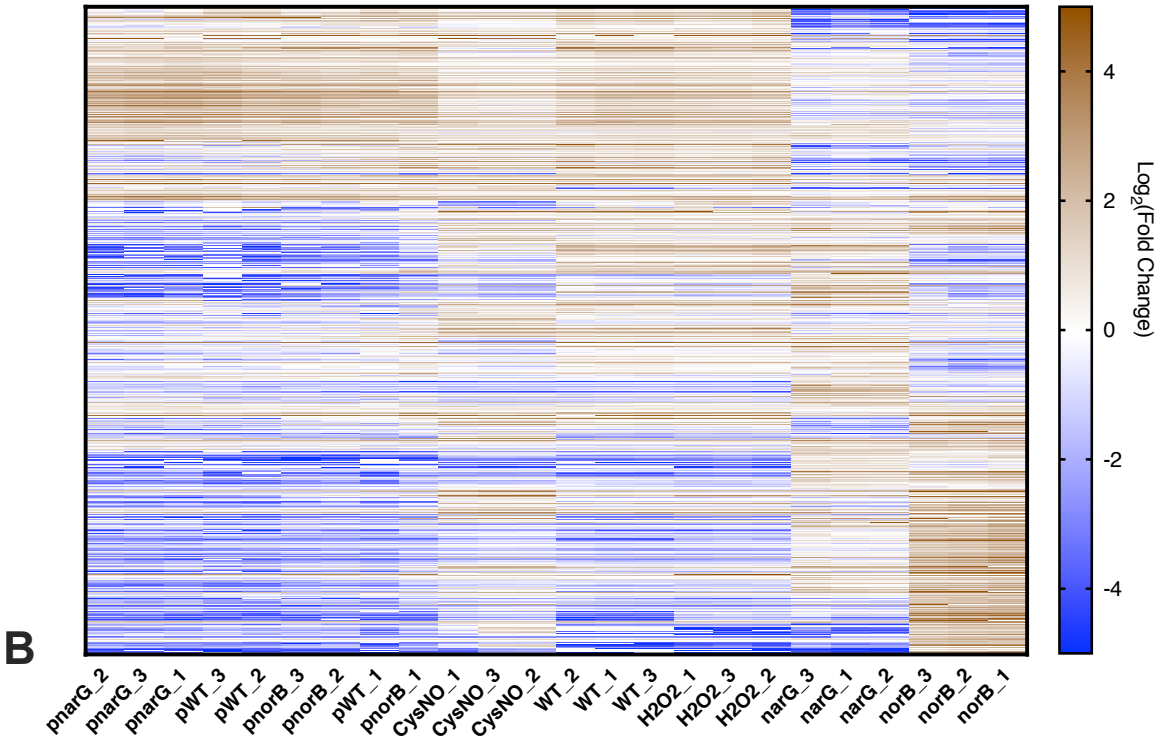
B
pnarG_2
pnarG_3
pnarG_1
pWT_3
pWT_2
pnorB_3
pnorB_2
pWT_1
pnorB_1
CysNO_1
CysNO_3
CysNO_2
WT_2
WT_1
WT_3
H2O2_1
H2O2_3
H2O2_2
narG_3
narG_1
narG_2
norB_3
norB_2
norB_1
4
2
0
-2
-4
Log_2(Fold Change)

922

923 **Supplementary Fig. 3.** General RNA-seq quality **A,** Total and mapped reads per RNA-
924 seq sample. The *in planta* samples had lower percentage of mapped reads due to the
925 presence of host RNA. **B,** Hierarchical clustering and expression heat map of the 1000
926 most variable genes in the dataset. Blue indicates higher expression and brown
927 indicates lower expression. All genes were normalized to the mean gene expression
928 across all conditions. Samples collected from *R. solanacearum* grown *in planta* are
929 denoted with the prefix "p". Heatmap created using iDEP.90 (Ge et al. 2018).
930
931 **Supplementary Table 2** Complete list of gene expression and $\log_2$ fold change values
932 for all conditions included in this study. All fold-change numbers are compared to levels
933 in untreated wild-type (WT) cells. NO levels were modified genetically using mutants
934 lacking *narG* (deleting this nitrate reductase reduces endogenous NO) and *norB*
935 (deleting this nitric oxide reductase increases endogenous NO). NO levels were
936 increased chemically by adding 1 mM CysNO. Cells treated with 100 μM hydrogen
937 peroxide (H_2O_2) were a non-NO control to identify general stress responses. *P*-values
938 were calculated by DESeq were adjusted to control for the false discovery rate (FDR)
939 using the Benjamini-Hochberg approach.
940
941 **Supplementary Table 3** KEGG enrichment of genes altered in each condition.
942 enrichment was calculated using KOBAS v2.0 software. *P* values were calculated using
943 a hypergeometric test and adjusted using the Benjamini and Hochberg FDR correction
944 method.

945

946 **Supplementary Table 4** Annotations, Log_2 fold change relative to wild-type and
947 adjusted p-values for *R. solanacearum* T3SS related genes in response to changes in
948 NO concentration both *in planta* and in culture (see Figure 3 for heatmap of these data).
949 All fold-change numbers are compared to levels in untreated wild-type (WT) cells. *in*
950 *planta* samples are denoted by a 'p' in front of the treatment (e.g. *pnorB*). Genes
951 organized by their category, including structural genes, regulatory genes, chaperones,
952 and effectors. Effectors are subgrouped based on their known association with
953 chaperones (Lonjon et al. 2015).